U.S. Department of Transportation
Federal Aviation Administration

FINAL PROJECT REPORT

Form Approved:
O.M.B. No. 2120-0559
9/30/2013

PART I - PROJECT IDENTIFICATION INFORMATION

1. Institution and Address	2. FAA Program	3. FAA Award Number
Georgia Institute of Technology	ASCENT 098	13-C-AJFE-GIT-142
620 Cherry Street, Atlanta, GA, 30332	4. Award Period From 08/11/20 To 09/30/24	5. Cumulative Award Amount 3099994

6. Project Title

Low emission premixed combustion technology for supersonic civil transport

PART II - SUMMARY OF COMPLETED PROJECT (For Public Use)

This project advanced the state-of-the-art in fuel-lean premixed prevaporized (LPP) combustor technology for use in future civil supersonic transport (CST) aircraft engines. Cruise conditions for CST aircraft are such that combustors operate in a different parameter space than combustors for traditional subsonic aircraft. These conditions lead to challenges meeting environmental targets, particularly regarding NOx. LPP combustors can enable step-change improvements in NOx emissions, but have different operability constraints and less mature design tools compared to current combustor architectures. This project partnered advanced test facilities, state-of-the-art laser diagnostics, high-fidelity numerical simulations, and reduced order modeling to gain new insight regarding LPP combustor performance and develop/validate design tools. A LPP combustor concept was designed, fabricated, commissioned, and tested. Laser diagnostics from were used to measure the velocity field, flame structure, fuel spray, fuel/air mixing, and other aspects of the combustor performance across operating conditions and with both conventional and sustainable aviation fuels. Emissions were in line with NASA's ambitious targets for future CST aircraft. Operability limits, flame structure, and combustion dynamics were well-explained by theoretical considerations and reduced order models. The experimental data provided quantitative benchmarks for simulations, and identified areas for fruitful model improvement.

PART III - TECHNICAL INFORMATION (For Program Management Uses)

1. **ITEM** (Check appropriate blocks)	NONE	ATTACHED	PREVIOUSLY FURNISHED	TO BE FURNISHED SEPARATELY TO PROGRAM	
				Check (X)	Approx. Date
a. Abstracts of Theses		✘			
b. Publication Citations		✘			
c. Data on Scientific Collaborators		✘			
d. Information on Inventions	✘				
e. Technical Description of Project and Results		✘			
f. Other (specify)					

2. Principal Investigator/Project Director Name (Typed)	3. Principal Investigator / Project Director Signature	4. Date
Adam Steinberg		5/1/2025

FAA Form 9550-5 (03-03) Supersedes Previous Edition

FAA ASCENT 074 Thesis Abstracts (Starting on Next Page)

FUEL DROPLET OPTICAL DIAGNOSTIC TECHNIQUES FOR LEAN PREVAPORIZED PREMIXED AEROENGINE COMBUSTORS

A Dissertation
Presented to
The Academic Faculty

By

Ijeoma Obi

In Partial Fulfillment
of the Requirements for the Degree
Masters of Science in the
Woodruff School
of Mechanical Engineering

Georgia Institute of Technology

May 2025

SUMMARY

Recent advancements in Civil Supersonic Transport (CST) have sparked interest in developing new technologies aimed at reducing the environmental impact of CST jet engines. Because these engines require lower pressure and bypass ratios, they tend to consume more fuel and produce higher emissions compared to their subsonic counterparts. One promising solution is the Lean Prevaporized Premixed (LPP) combustor design, which shows potential for lowering emissions at supersonic conditions. However, further experimental research are required to fully understand these combustors. Key areas of focus include analyzing fuel droplets with these combustors across various operating conditions relevant to CST.

To further assist with ongoing research and support for the future design of LPP combustors, this study employs a combination of diagnostics: Mie scattering, Holography and direct imaging with Shadowgraphy — to enhance the understanding of fuel spray dynamics in LPP combustors. Both Jet-A and Sustainable Aviation Fuel (SAF), specifically, a Hydrotreated Esters and Fatty Acids (HEFA) fuels were studied to compare their spray characteristics under varying operating conditions. Mie scattering is utilized to visualize spray, aiding in the identification of optimal positions for hologram capture. Two holographic imaging techniques, long-standoff Digital Inline Holography (DIH) and Digital Off-axis Holography (DOH), are compared to measure fuel droplet sizes at the dome face of the combustor. These techniques are evaluated based on their effectiveness in eliminating distortions caused by thermal gradients. Finally, Shadowgraphy is employed to observe and analyze liquid fuel droplets. The findings aim to inform the future design of LPP combustors for CST jet engines, contributing to more efficient and environmentally friendly supersonic engines.

AN EXPERIMENTAL CHARACTERIZATION OF A MULTI-ELEMENT LEAN PREMIXED PRE-VAPORIZED COMBUSTOR FOR SUPERSONIC TRANSPORT APPLICATIONS

A Dissertation
Presented to
The Academic Faculty

by

Mitchell Louis Passarelli

In Partial Fulfillment
of the Requirements for the Degree
Doctor of Philosophy in the
School of Aerospace Engineering

Georgia Institute of Technology

December 2023

SUMMARY

Recent trends have driven a re-emergence of research and development in aircraft engines for commercial supersonic transport (CST). Despite the vast body of literature that exists for gas turbine combustors operating at conditions relevant to conventional subsonic flight, there is little to validate extensions of this knowledge to the conditions encountered by CST engines. Further complications arise from advanced combustor designs that involve multiple different flames or flow devices. The interactions of such combustor elements can lead to individual behaviours that differ from that of single elements.

The existing literature on flame and flow interactions is focused on conditions relevant to the operation of conventional, subsonic aircraft engines. While such works provide a baseline understanding of the physical phenomena involved in such interactions, they do not necessarily predict the behaviours exhibited by different combustor configurations and/or at different conditions. Some recent studies have employed numerical simulations to determine the characteristics of various combustor schemes, including lean direct injection and lean premixed pre-vaporized (LPP) designs. These studies are limited by the lack of empirical data for validation and model development.

The work presented herein aims to characterize experimentally the flow field, flame dynamics and operating limits of a multi-element LPP combustor operating at CST-relevant conditions. Simultaneous laser and probe-based diagnostics were employed to obtain measurements of pollutant emissions, flow velocities, heat release rate, fuel-air mixing and thermoacoustic dynamics. The effects of combustor inlet pressure, temperature and fuel-air ratio are studied via corresponding parameter sweeps. Numerical chemistry simulations

provide estimates of relevant flame properties, complementary to the experimental results. A second set of experiments investigated the forced response of the combustor.

Overall, the results presented in this thesis demonstrate the importance of flame and flow interactions. In particular, the interactions of the pilot flame with neighbouring main flames are found to be critical in determining the stable operating range of the combustor. Furthermore, the pilot is found to dominate the dynamics of the combustor at forced and unforced conditions. Empirically-computed flame transfer functions at different forcing frequencies show that the pilot is most sensitive to acoustic perturbations and that this sensitivity is enhanced by interactions of the pilot with the main flames.

This work also demonstrates the viability of LPP combustors for CST applications in three aspects. First, the pollutant emissions characteristics of the combustor studied are in line with future emissions targets. Second, the mean flow field, flame and dynamical characteristics do not vary strongly with operating conditions or undergo sudden or unexpected bifurcations, except when exceeding blowoff limits. A Damköhler number (Da)-based blowoff analysis shows that this combustor design exhibits enhanced stability compared with previously reported bluff-body stabilized flames. The analysis itself also demonstrates the robustness of a simple Da correlation for blowoff prediction, which works for a complex geometry such as the one studied in this work.

CHARACTERIZATION OF NON-VOLATILE PARTICULATE MATTER IN PRESSURIZED PREMIXED LAMINAR JET-A FLAMES VIA THERMOPHORETIC SAMPLING

A Dissertation
Presented to
The Academic Faculty

By

Sundar Ram Manikandan

In Partial Fulfillment
of the Requirements for the Degree of
Master of Science in
Aerospace Engineering
Daniel Guggenheim School of Aerospace Engineering

Georgia Institute of Technology

August 2022

SUMMARY

Production and subsequent emissions of non-volatile particulate matter (nvPM) pose a challenge for both optical diagnostics and physical probing, especially at conditions relevant to practical combustors. Key to enabling nvPM mitigation is *in-situ* optical measurements, particularly laser induced incandescence (LII). However, interpreting the LII signals is challenging. To quantitatively use LII in gas turbines, their measurements must be calibrated and validated against physical nvPM samples. The preferred approach for extracting these physical samples is *in-situ* thermophoretic soot sampling followed by transmission electron microscope (TEM) imaging.

This thesis work deals with the design of a multi-probe thermophoretic soot sampling system capable of extracting nvPM samples in laminar, rich flames of prevaporized jet-A/air premixtures at elevated pressures. The flames under investigation were observed to exhibit thermal-diffusive instabilities, that are responsible for the flame to form corrugated structures. Moreover, these instabilities cause the corrugated flame to exhibit spatio-temporal variations, which exacerbate the challenges in implementing diagnostics. For the soot sampler, a significantly larger sampling time of 125 ms was required to obtain sufficient soot deposition on the TEM grids, which can enhance the extent of restructuring in the deposited soot particles.

Visualization of the data through the TEM revealed (i) a wide range of soot particle size varying between 10 – 250 nm; (ii) presence of non-soot organic matters that include (1) fibers, (2) sharp contrasted mineral-like structures, and (3) uniform and porous spherical structures with varying contrast; and (iii) the dominant morphological characteristics of the flame generated soot particles that are indicative of its chemically reactive nature and restructuring. Furthermore, the quantitative results show (i) increasing soot particle size with pressure, and (ii) an increasing-decreasing trend for the mean soot particle size with height above the burner. While the effect of pressure is explained by the enhanced extent

of graphitization and maturity in the nanostructures of soot particles at elevated pressures; the dependence on height can be explained through particle agglomeration for the initial increase in size with height, followed by oxidation of the particles respectively. However, considering the range of tested HAB when compared to the flame length, the possibility for inconclusive variation stems from preheat temperature variations and restructuring effects.

FAA ASCENT 074 Publication Citations

A. Jain, I. Obi, Y.C. Mazumdar, V. Salazar, M. Kodali, K. Venkatesan, A. M. Steinberg, "Flame Structure, Spray, and Blowout of a Lean Premixed Prevaporized Combustor With Conventional and Sustainable Jet Fuels," *AIAA Journal*, Submitted (2025)

A. Jain, I. Obi, Y.C. Mazumdar, V. Salazar, M. Kodali, K. Venkatesan, A. M. Steinberg, "Flame Structure, Spray, and Blowout of a Lean Premixed Prevaporized Combustor With Conventional and Sustainable Jet Fuels," *AIAA SciTech Forum*, AIAA-2025-0791 (2025)

M. L. Passarelli, S. E. Wonfor, A. X. Zheng, Y.-C. Mazumdar, A. M Steinberg, H. Bower, J. Hong, K. Venkatesan, "Blowoff Characteristics of a Bluff-Body Stabilized, Multi-Element, Lean Premixed Pre-Vaporized Combustor for Supersonic Transport Applications," *ASME Turbo Expo*, GT2024-129322 (2024)

A. X. Zheng, S. R. Manikandan, S. E. Wonfor, A. M. Steinberg, Y. C. Mazumdar, "Planar time-resolved laser-induced incandescence for pressurized premixed Jet-A combustion," *Applied Physics B*, 129:71 (2023)

V. Salazar, K. Venkatesan, F. Han, S. Wonfor, M. Passarelli, A. Zheng, A. Steinberg, "Acoustic and optical flame transfer function measurements in a high-pressure lean-burn aero-engine combustor fueled with Jet A," *ASME Turbo Expo*, GT2023-10322 (2023)

A. X. Zheng, S. Manikandan, S. E. Wonfor, A. M. Steinberg, Y. C. Mazumdar, "Planar time-resolved laser-induced incandescence for particulate emissions in premixed flames at elevated pressures," *AIAA SciTech Forum*, AIAA 2023-2435 (2023)

M. L. Passarelli, S. E. Wonfor, A. X. Zheng, Y. C. Mazumdar, J. M. Seitzman, A. M. Steinberg, V. Salazar, K. Venkatesan, M. Benjamin, "Forced and Unforced Dynamics of a Lean Premixed Prevaporized Combustor for Civil Supersonic Transport," *AIAA SciTech Forum*, AIAA 2023-0920 (2023)

M. L. Passarelli, S. E. Wonfor, A. X. Zheng, S. R. Manikandan, Y. C. Mazumdar, J. M. Seitzman, A. M. Steinberg, H. Bower, J. Hong, K. Venkatesan, M. Benjamin, "Experimental characterization of a lean prevaporized premixed combustors for supersonic transport applications," *AIAA SciTech Forum*, AIAA 2022-2347 (2022)

Data on Scientific Collaborators

Name	Affiliation	Role	Tasks
Adam Steinberg Professor	Georgia Institute of Technology	P.I.	Management, reporting, technical oversight of all tasks, oversight of optical diagnostics in Task 1
Ellen Mazumdar Assistant professor	Georgia Institute of Technology	Co-P.I.	Oversight of OH PLIF measurements in Task 1
Joseph Oefelein Professor	Georgia Institute of Technology	Co-P.I.	Oversight of first-principles LES in Task 2 and overall coordination of Task 2
Jerry Seitzman Professor	Georgia Institute of Technology	Co-P.I.	Oversight of gas phase fuel/air mixing diagnostics in Task 1
Michael Benjamin Consulting engineer	GE Aviation	Co-P.I.	Oversight of combustor design in Task 1, coordination of GT/GE LES collaboration in Task 2
Krishna Venkatesan Principal engineer	GE Research	Co-P.I.	Oversight of combustor operation in Task 1 and data collection for Task 3
Oleksandr Bibik Senior research scientist	Georgia Institute of Technology	Participant	Task 1
Hannah Bower Research engineer	GE Research	Participant	Task 1
Fei Han Engineering manager	GE Research	Participant	Task 3
John Hong Lead engineer	GE Research	Participant	Task 1
Nick Magina Lead engineer	GE Research	Participant	Task 3
Victor Salazar Lead engineer	GE Research	Participant	Task 1
R. Narasimha Chiranthan	GE Aviation	Participant	Task 2

Manampathy Giridharan	GE Aviation	Participant	Task 2
Hiranya Nath	GE Aviation	Participant	Task 2
Sriram Kalathoor Graduate research assistant	Georgia Institute of Technology	Graduate student	Task 2
Arihant Jain Graduate research assistant	Georgia Institute of Technology	Graduate student	Task 1
Ijeoma Obi Graduate research assistant	Georgia Institute of Technology	Graduate student	Task 1
Mitchell Passarelli Graduate research assistant	Georgia Institute of Technology	Graduate student	Task 1
Sundar Ram Manikandan Graduate research assistant	Georgia Institute of Technology	Graduate student	Task 1
Samuel Wonfor Graduate research assistant	Georgia Institute of Technology	Graduate student	Task 1
Andrew Zheng Graduate research assistant	Georgia Institute of Technology	Graduate student	Task 1
Neilay Amin Research assistant	Georgia Institute of Technology	Undergrad student	Task 2
Preethi Mysore Research assistant	Georgia Institute of Technology	Undergrad student	Task 2
Coleman Pethel Research assistant	Georgia Institute of Technology	Undergrad student	Task 1
Katrina Potak Research assistant	Georgia Institute of Technology	Undergrad student	Task 2
Mihir Rao Research assistant	Georgia Institute of Technology	Undergrad student	Task 1
Andrew Semelka Research assistant	Georgia Institute of Technology	Undergrad student	Task 1
Rachel Wilder Research assistant	Georgia Institute of Technology	Undergrad student	Task 2

Project 074 Low Emissions Premixed Combustion Technology for Supersonic Civil Transport

Georgia Institute of Technology

Project Lead Investigator

Adam Steinberg
Professor
School of Aerospace Engineering
Georgia Institute of Technology
Phone: (404) 897-1130
E-mail: adam.steinberg@gatech.edu

University Participants

Georgia Institute of Technology (Georgia Tech)

- P.I.: Prof. Adam Steinberg, School of Aerospace Engineering
- FAA Award Number: 13-C-AJFE-GIT-142
- Period of Performance: August 11, 2020, to September 30, 2024
  Period of Performance Covered in Report: October 1, 2023, to September 30, 2024
- Tasks:
  1. Execution of Experimental Campaign 3, performing hydroxyl (OH) Planar Laser Induced Fluorescence (PLIF), Mie scattering, and Phase Doppler Particle Analyzer (PDPA) measurements with conventional and alternative fuels
  2. Data analysis to determine fuel properties, droplet sizes, evaporation lengths, flame surface densities, and lean blow-out (LBO) limits

Project Funding Level

The Federal Aviation Administration (FAA) provided $3,102,994 in funding. Cost-sharing is provided by Georgia Institute of Technology ($1,544,950) and GE® Research ($1,558,044).

Investigation Team

Georgia Institute of Technology

Prof. Adam Steinber (P.I.), Management, reporting, technical oversight of all tasks, oversight of optical diagnostics in Task 1.
Ellen Mazumdar (Co-P.I.), Assistant Professor, Oversight of OH PLIF measurements in Task 1.
Prof. Joseph Ofelein (Co-P.I.), Oversight of first-principles LES in Task 2 and overall coordination of Task 2.
Prof. Jerry Seitzman (Co-P.I.), Oversight of gas phase fuel/air mixing diagnostics in Task 1.
Oleksandr Bibik, Senior Research Scientist, Task 1
Mitchell Passarelli, Graduate Research Assistant, Task 1
Sundar Ram Manikandan, Graduate Research Assistant, Task 1
Samuel Wonfor, Graduate Research Assistant, Task 1
Andrew Zheng, Graduate Research Assistant, Task 1
Arihant Jain, Graduate student, Task 1
Ijeoma Obi, Graduate student, Task 1
Sriram Kalathoor, Graduate Research Assistant, Task 2
Coleman Pethel, Research Assistant (Undergraduate student), Task 1
Mihir Rao, Research Assistant (Undergraduate student), Task 1

® GE is a registered trademark of General Electric Company, Schenectady, New York.

Andrew Semelka, Research Assistant (Undergraduate student), Task 1
Neilay Amin, Research Assistant (Undergraduate student), Task 2
Preethi Mysore, Research Assistant (Undergraduate student), Task 2
Katrina Potak, Research Assistant (Undergraduate student), Task 2
Rachel Wilder, Research Assistant (Undergraduate student), Task 2

GE Research

Krishna Venkatesan (Co-P.I.), Principal Engineer, Oversight of combustor operation in Task 1 and data collection for Task 3.
Hannah Bower, Research Engineer, Task 1
Fei Han, Engineering Manager, Task 3
John Hong, Lead Engineer, Task 1
Nick Magina, Task 3
Victor Salazar, Lead Engineer, Task

GE Aviation

Michael Benjamin (Co-P.I.), Consulting Engineer, Oversight of combustor design in Task 1, coordination of GT/GE LES collaboration in Task 2.
R. Narasimha Chiranthan, Task 2
Manampathy Giridharan, Task 2
Hiranya Nath, Task 2

Project Overview

Market demand for high-speed transport is expected to drive a rapid re-emergence of commercial supersonic transport (CST) aircraft over the coming decades. This impending CST revival and the increasingly harmful impacts of anthropogenic climate change mandate advancements in CST-focused environmentally compatible technologies and policies. Compared with subsonic aircraft, engines for CST aircraft will (a) operate at significantly lower overall pressure ratio (OPR) and bypass ratio (BR), (b) experience higher combustor inflow temperatures (T_3), lower pressures (p_3), and higher fuel/air ratios (FAR) at cruise, and (c) cruise at higher altitudes. The reduced OPR and BR result in increased thrust-specific fuel consumption, thus increasing fuel burn and making it fundamentally more challenging to reduce emissions. Furthermore, the combination of low OPR and high cruise T_3 and FAR result in complicated trade-offs between nitrogen oxides (NO_x) at cruise and other emissions (carbon monoxide [CO], nonvolatile particulate matter [nvPM] and unburnt hydrocarbons [UHC]) at lower power.

Several recent studies have assessed potential CST fleet emissions and environmental impact based on currently deployed rich burn-quench-lean burn combustors (typically Tech Insertion combustors) designed for subsonic transports (Kharina et al., 2018; Berton et al., 2020; Hassan et al., 2020; Speth et al., 2021). These studies demonstrate that innovations in combustor architecture will be required to meet emissions and efficiency targets, helping enable an environmentally compatible CST market. Despite the high T_3 and FAR, peak flame temperatures must be moderated to meet NO_x targets, while also maintaining efficiency and achieving low CO, UHC, and nvPM. This will require increased fuel-lean premixing before combustion.

Lean premixed prevaporized (LPP) combustors are a promising path to lowering emissions from future CST engines. In LPP, fuel is injected, partially prevaporized and partially premixed with air before the reactants enter the combustor. While the concept of LPP is not new (e.g., Niedzwiecki, 1992), achieving good vaporization and mixing in a flight-appropriate package previously has been challenging. However, these issues can potentially be alleviated by the high T_3 in CST combustors (which results in faster vaporization) and advanced manufacturing to enable compact rapid-mixing flow elements.

However, the ability of current design methodologies to predict the operability and emissions of LPP combustors under relevant conditions is unproven. Hence, there is a critical need to generate high-quality experimental data at CST combustor conditions, coupled with the development/validation of computational fluid dynamics (CFD) simulations and reduced-order thermoacoustic models. This project addresses this need through a combination of experiments, large eddy simulations (LES), and thermoacoustic modeling, all applied in a novel LPP combustor of interest to future CST applications. This report focuses on analysis of LBO and thermoacoustic dynamics, the majority of which was performed by PhD candidate Mitchell Passarelli.

Task 1- Analysis of Combustor Performance with Conventional and Alternative Fuels

Georgia Institute of Technology

Objectives

The overarching objectives of Task 1 were to (1) demonstrate the operability of the LPP combustor at the conditions of interest, including demonstrating the potential to hit National Aeronautics and Space Administration (NASA) long-term NO_x goals for supersonic cruise, (2) measure and understand any thermoacoustic dynamics in this combustor, (3) measure and understand the process of LBO in this combustor, (4) measure and understand the impact of using sustainable aviation fuel (SAF) in this combustor, and (5) provide quantitative data with which to develop and validate predictive models, particularly LES and thermoacoustic solvers. Objectives (1) and (2) were fully achieved during the previous reporting periods. Objectives (3) and (5) were largely completed during previous reporting periods. The focus of the last reporting period was on the impact of SAFs, including collection of additional LBO boundaries and extensive data for validation of LES with both conventional fuels and SAF.

Research Approach

1. Experiment

1.1 Configuration and Operating Conditions

Experiments were conducted at GE Research in Niskayuna, New York, in a lean premixed prevaporized combustor that has been detailed in previous studies (Passarelli et al., 2024; Passarelli et al., 2023; Passarelli et al., 2022; Salazar et al., 2023). Figure 1a shows a conceptual schematic of the combustor dome face, which contains four bluff-body stabilized LPP main flames surrounding a non-premixed swirling pilot. Figure 1b shows the side view, with a simplified flow field adapted from (Lovett et al., 2011). For the optical diagnostics measurements, quartz windows were used for the side and top walls of the combustor. The combustor bottom wall is optically inaccessible, as it houses the ignitor.

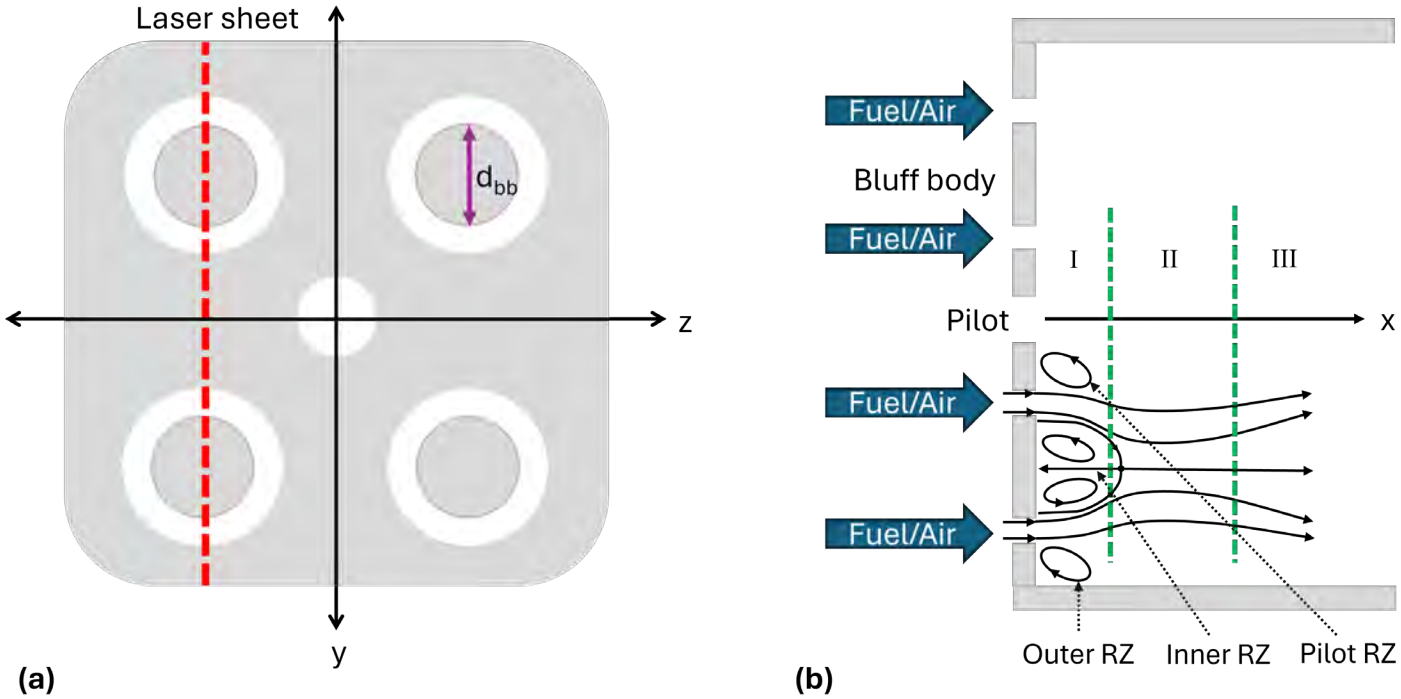

Figure 1. Schematic of combustor dome face (a) and side view of notional flow field (b).

Three liquid fuel lines supply the combustor, one to the pilot and the other two to the top and bottom mains flames. A torch ignitor is located inside the combustor to ignite the fuel-air mixture. All the air, fuel, and water flows to the test rig are individually metered and controlled. Within the mixer are discrete fuel injectors arranged azimuthally, and the angular

positions of these injectors vary slightly from main-to-main. The operating conditions of the combustor for the majority of experiments are detailed in Table 1. The FAR sweep targets four nominal conditions tested at all air preheat temperatures T_3. A finer FAR sweep also is performed to precisely identify the LBO conditions, with the specific FAR values depending on T_3. The exact values of T_3 are not provided here but instead normalized by a reference temperature $T_{3,\mathrm{ref}}$. $T_{3,\mathrm{ref}}$ is in a range that results in significant, but not complete, fuel pre-vaporization. FAR varies by keeping air mass flow rate constant while changing fuel mass flow rate. The pilot is kept at an equivalence ratio of $\phi = 1$.

Table 1. Test condition summary.

Parameter	Values		
Fuel	100% SAF, 100% Jet A, 50/50 volumetric blend		
Reactant pressure p_3 (bar)	7.9		
Nominal FAR of mains	0.055, 0.050, 0.045, 0.040		
Reactant temperature T_3	$0.93T_{3,\mathrm{ref}}$	$T_{3,\mathrm{ref}}$	$1.10T_{3,\mathrm{ref}}$
LBO Sweep Main FAR	0.046, 0.044, 0.043, 0.042	0.044, 0.043, 0.042, 0.041	0.042, 0.041, 0.039

The SAF used in this work is a hydrotreated esters and fatty acids (HEFA) fuel manufactured by World Energy®. HEFA fuel distillation profiles mimic those of the petroleum-derived jet fuels (C8 to C16 hydrocarbons), but their distribution may differ. In terms of chemical composition, HEFA fuels are primarily composed of saturated n-paraffins and isoparaffins with negligible aromatics or cycloparaffins (Vozka et al., 2018). In comparison, Jet A fuel aromatic and cycloparaffinic content is typically around 18% and 30%, respectively.

Samples of fuels used in this study were analyzed by the National Renewable Energy Laboratory (NREL) to determine physical and chemical properties, which are presented in Table 2. The values marked with an asterisk are not yet measured, and thus are calculated from literature correlations (EPA, 2007). All fuel properties comply with ASTM D1655 standards (ASTM International, 2023), except for the 100% SAF density. Lack of aromatics contributes to a higher hydrogen/carbon (H/C) ratio and lower heating value (LHV) for the HEFA, which is expected to yield less soot formation and lower fuel mass consumption rates, respectively. Other measured properties included freeze and flash point, and distillation curves, which are omitted for succinctness but also complied with standards.

Table 2. Fuel chemical and physical properties. ICN: Indicated cetane number.

Property	HEFA	Blend	Jet A
Density (g/cm3) at 288 K	0.747	0.775	0.793
ICN	59.5	54.3	48.6
LHV (MJ/kg)	44.0*	43.6*	43.3
Viscosity (mm2/s) at 258 K	4.140	4.827	3.613
H/C ratio	2.15	2.03	1.92
Vapor pressure (kPa) at 311 K	3.04	2.84	2.62
Surface tension (mN/m) at 295 K	23.72	24.77	25.85
ASTM D86 distillation temperature at 10% recovered (K)	437	445	458

® World Energy is a registered trademark of World Management Group, LLC, Boston, Massachusetts.

ASTM D86 distillation temperature at 90% recovered (K)	524	523	521

1.2 Optical Diagnostics

1.2.1 OH Planar Laser Induced Fluorescence (PLIF)

In OH PLIF, a laser is used to excite OH radicals, and their subsequent fluorescence is captured using an intensified camera. OH exists at detectable quantities in product gases at temperatures above about 1550 K; in premixed flames, the OH PLIF signal is a good demarcation of the flame surface topology (Sweeney & Hochgreb, 2009; Carter & Lee, 2022).

OH PLIF was stimulated by using a neodymium-doped yttrium aluminum garnet (Nd:YAG) laser (EdgeWave™ InnoSlab IS300-2-L, 532 nm, 10 kHz, 10 mJ/pulse) to pump a tunable dye laser (Sirah™ Rhodamine 6G). The dye laser output at approximately 566 nm was frequency-doubled to yield an ultraviolet (UV) pulse with energy of approximately 340 µJ. The dye laser output was tuned to excite the Q1(9) transition of OH in the $A^2\Sigma^+ - X^2\Pi(1,0)$ band near 283.9~nm (Saini et al., 2020; Fugger et al., 2020).

The optics used to form the laser sheet and transmit it into the combustor are shown in Figure 2. The laser sheet is positioned along the centerline of one set of mains, as shown in Figure 1a. The sheet is 50 mm long with a beam waist of approximately 1 mm. As shown in Figure 2, the residual sheet that does not get reflected into the test section is impinged on a phosphor-coated plate placed after the final mirror. The resultant phosphorescence is imaged by a camera (FLIR Blackfly®) with a colored glass filter. This camera captured 100 PLIF laser pulses per test point, enabling a mean laser sheet intensity profile correction.

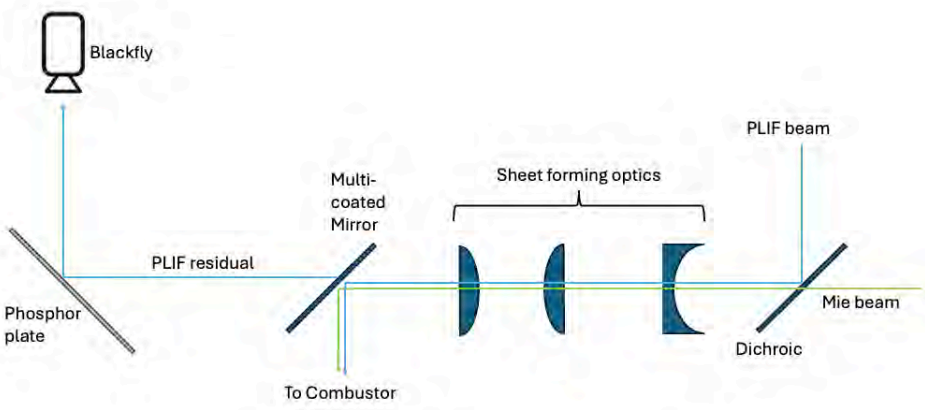

Figure 2. Simplified schematic of optical layout.

Images were recorded using a 308±10 nm filter, UV objective lens (Cerco™ 100 mm, f/# = 2.8) and a high-speed camera (Photron® SA-5) coupled to an image intensifier (Invisible Vision™ UVi 2550B-10, gate time of 100 ns, 896 x 848 pixels). The camera recorded 15,068 frames (1.5068 s) per test point with a projected pixel size of 119.2 micron/pixel. The limiting spatial resolution of the PLIF system is expected to be set by signal integration across the depth of the ca. 1 mm laser sheet thickness, particularly in the highly turbulent wrinkled flames studied here.

™ Edgewave is a trademark of EdgeWave GmbH, Germany.
™ Sirah is a trademark of Sirah Lasertechnik GmbH, Germany.
® Blackfly is a registered trademark of Teledyne FLIR, Wilsonville, Oregon.
™ Cerco is a trademark of Cercolens, France.
® Photron is a registered trademark of Photron Limited, Tokyo, Japan.
™ Invisible Vision is a trademark of Invisible Vision Limited, United Kingdom.

1.2.2 Fuel Droplet Mie Scattering

Mie scattering was used to qualitatively describe the fuel sprays and their downstream penetration. Mie scattering from the fuel droplets was generated from the output of an Nd:YAG laser (Quantel® Evergreen EVG00200, 532 nm, 10 Hz, 160 mJ/pulse). The Mie laser sheet optics also are shown in Figure 2. Data were acquired using a high-speed camera (Phantom® v7.3) due to its low minimum exposure time, though not all frames contained Mie scattering data from the 10 Hz laser. For each test point, 1184 frames with Mie scattering were collected at an exposure of 1μs.

1.2.3 Phase Doppler Particle Analysis

A TSI® Flow and Size Analyzer (FSA) 3500 two-component Phase Doppler Interferometer system was utilized to measure local droplet size and velocity parallel and radial to the mixer axis during operation. For these tests, measurements were performed only at $T_{3,\mathrm{ref}}$ (FAR = 0.040 and 0.050) and $1.10T_{3,\mathrm{ref}}$ (FAR = 0.050). All the measurements were performed at the main tubes plane as depicted in Figure 1a. Since the PDPA is a single point measurement, mapping the entire spray region is quite time consuming. Therefore, in this campaign, vertical scans at two select axial locations: $x = 1$ mm and $x = 10$ mm from the mixer face, were only performed.

2. Data Analysis Techniques

2.1 Flame Surface Density

Flame surface density (FSD) is of fundamental interest in premixed turbulent combustion and defined as the reaction layer surface layer per unit volume:

$$\Sigma_{3\mathrm{D}} = \lim_{\Delta x \to 0} \frac{A_{\mathrm{T}}}{\Delta x^3} \qquad \text{(Eq. 1)}$$

where $\Delta x$and A_{T}re interrogation box side length and wrinkled flame surface area, respectively (Candel & Poinsot, 1990). In planar measurements, it is common to approximate the FSD as the flame perimeter per unit area in the laser sheet:

$$\Sigma_{2\mathrm{D}} = \frac{L_{\mathrm{T}}}{\Delta x^2} \qquad \text{(Eq. 2)}$$

for small Δx. The accuracy of the two-dimensional (2D) approximation has been experimentally shown to be in reasonable agreement with three-dimensional (3D) measurements, though a multiplicative factor is needed to quantitatively align 2D and 3D FSD data (Filatyev et al., 2005; Han et al., 2018; Bell et al., 2007). Here, we are concerned with FSD spatial distributions and trends with operating conditions/fuels, which do not require consideration of such factors.

While there are multiple definitions of the flame front, location of peak heat release is generally accepted as a common standard (Sweeney & Hochgreb, 2009). This location tends to approximate coincident with the point of maximum gradient in both temperature and OH concentration. In ideal unstretched laminar flame calculations, OH concentration rises from zero in the unburned reactants to a peak within the flame front, before relaxing to the equilibrium product concentration (Sweeney & Hochgreb, 2009). However, experimental data are confounded by multiple factors, such as temperature dependence, signal quenching, noise, and spatial resolution. In instantaneous images, there can be significant noise from the intensifier and laser profile variability. The location of the maximum gradient along a flame surface may also vary due to local stoichiometry in flames will local composition variations (Chaib et al., 2023). High pressure gas turbine environments cause signal quenching and highly convoluted turbulent flames that are difficult to identify in image processing. This study defines the flame front as the location of peak OH signal gradient, as it is clear that regions with no signal mark no reaction or products.

Several steps are required to reliably determine a flame surface topology from OH PLIF images in the high-pressure, partially premixed flames studied here. Initial image processing steps include spatial calibration, cropping, background subtraction, flat-field intensifier response correction, and a beam profile correction. To calculate FSD, the OH PLIF images undergo a preprocessing algorithm followed by edge detection in MATLAB.® In general, one desires an algorithm to maximize tradeoffs between computational expense and supervision, without sacrificing accuracy. The preprocessing algorithm requires tuning of two main thresholding parameters, which is comparable to other algorithms in the literature

® Quantel is a registered trademark of Lumibird, France.
® Phantom is a registered trademark of Vision Research, Inc., Wayne, New Jersey.
® TSI is a registered trademark of TSI Incorporated, Shoreview, Minnesota.
® Matlab is a registered trademark of The Mathworks Inc., Natick, Massachusetts.

(Chaib et al., 2023). Here, edge detection utilizes the Canny method (Canny, 1986), which is broadly used across the combustion field, but introduces another thresholding tuning parameter.

Due to absorption of laser energy as the laser sheet traversed the combustor from top to bottom, the OH PLIF signal-to-noise ratio was higher in the upper portion of the combustor, as shown in Figure 3. Therefore, flame surfaces and FSD are only analyzed in the upper half of the combustor. While the combustor exhibits some asymmetry in operation, the general flame behavior is assumed to be similar in each main. FSD fields are calculated using a 5 x 5-pixel (0.59 x 0.59 mm) window. This window is swept over all pixels in an image to calculate FSDs centered at each pixel, followed by a temporal average of all images for a test point. Tuning parameters and window size were selected via a sensitivity study and kept consistent across test points.

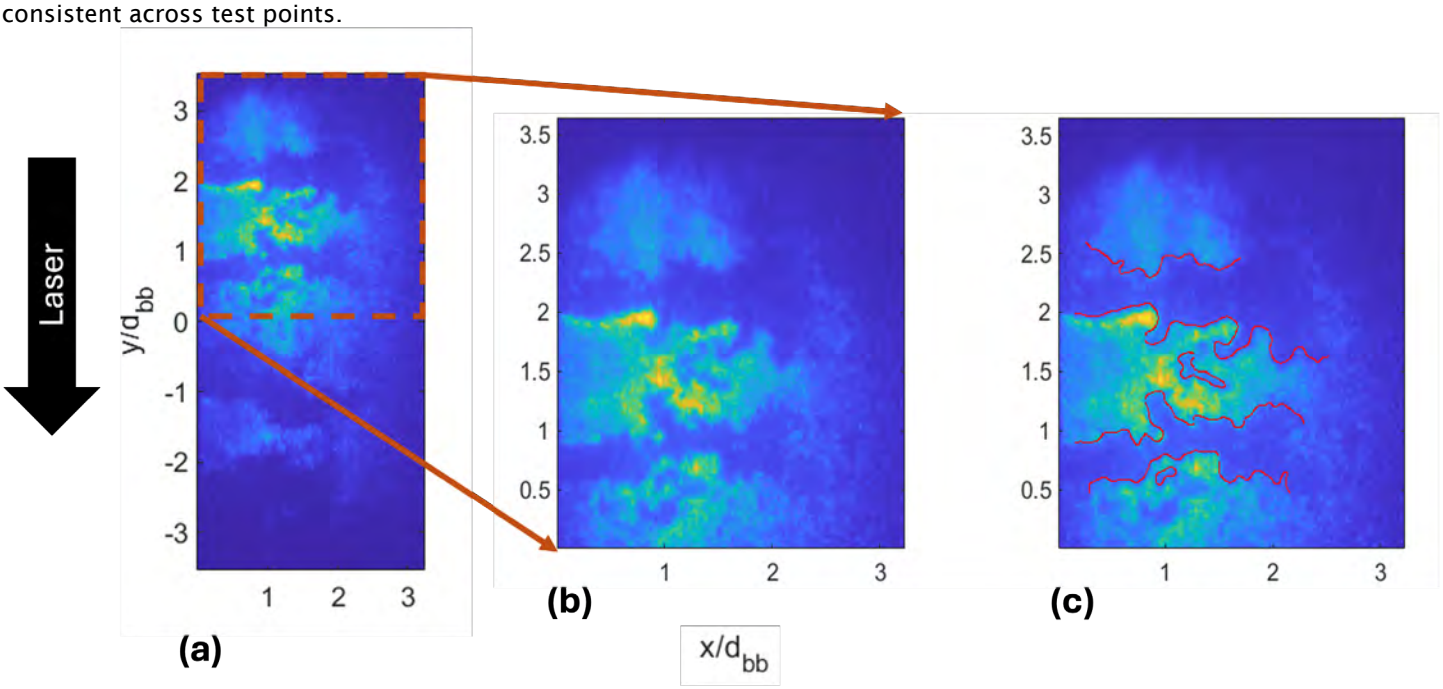

Figure 3. Example implementation of edge finding algorithm. (a) Raw image, (b) isolated region of interest from pilot midplane to top of the combustor, and (c) application of edge detection algorithm. Coordinates are normalized by bluff body diameter. Flow progresses from left to right.

2.2 Fuel Penetration Depth

To determine fuel depth penetration, x_{dp}, Mie scattering images first undergo dark-field and background subtraction. Additionally, due to soot deposition on the windows over the testing day, thresholding is applied to the areas impacted by the residues. To remain consistent with PLIF analysis, only the top main is analyzed. After preprocessing, pixel values are averaged along the y-axis. The axial coordinate at 30% of the maximum mean intensity is defined as x_{dp}.

2.3 Blow-off Characterization

LBO limits in bluff-body flames previously have been reviewed in Shanbhogue et al. (2009) and Tuttle (2010). Blow-off occurs due to competition between flow and chemical time scales, which is captured by Damköhler vs. Reynolds number correlations. The blow-off process is multifaceted, and complications can arise from chemical and aerodynamic interactions in multi-element combustors. Nonetheless, Damköhler number correlations have been shown to do a good job of collapsing LBO data across different combustors (Shanbhogue et al., 2009; Cavaliere et al., 2013).

The blow-off process described by Shanbhogue et al. (2009) is divided into two stages. In the first stage, as the Damköhler number in a stable flame is decreased, the local strain rate intermittently exceeds the extinction strain rate, creating holes in the flame from local extinction events. In the second stage, decreasing Damköhler number further causes more frequent extinction events, and the holes in the flame sheet lead to larger scale disruptions like flame flapping. Finally, further decrease of Damköhler number leads to blow-off.

Calculation of blow-off Damköhler and Reynolds numbers in this work follows the methodology from Passarelli et al. (2024). Reynolds number is computed as:

$$\mathrm{Re} = \frac{\rho_3 u_{\mathrm{main}} d_{\mathrm{bb}}}{\mu_3} \quad \text{(Eq. 3)}$$

where ρ_3 and μ_3 are the reactant mixture density and viscosity, respectively, assuming perfectly mixed, completely vaporized fuel and air. The characteristic flow speed, u_{main}, is computed from the one-dimensional (1D) continuity equation using the total mass flow rate through a single main. Damköhler number is defined as $\mathrm{Da} = \tau_{\mathrm{f}}/\tau_{\mathrm{c}}$, where the flow timescale τ_f is calculated using the empirical correlation for laminar boundary layer momentum thickness (Shanbhogue et al., 2009):

$$\tau_{\mathrm{f}} = \frac{35 d_{\mathrm{bb}}}{u_{\mathrm{main}} \mathrm{Re}^{1/2}} \quad \text{(Eq. 4)}$$

and the chemical timescale τ_c is calculated as the ratio of the unstretched laminar flame thermal thickness δ_{f}^0 and speed S_{L}^0.

Numerical simulations in Cantera[1] using the 1D freely propagating premixed laminar flame model were used to determine the flame and thermodynamic properties. Surrogate blends were used to model the tested fuels. The HEFA was modeled using pure n-dodecane (Liang et al., 2024); the Jet A fuel used n-dodecane/iso-octane/toluene 42.7/33.0/24.3 mol% (Dooley et al., 2010); and the blend used a 50/50 mix of its constituent surrogate components. The Chemical Reaction Engineering and Chemical Kinetics (CRECK) surrogate kerosene mechanism for low and high temperature kinetics, which has been extensively validated and implemented across the literature, is used for all fuels (Ranzi, 2014). Blow-off conditions are defined from the OH PLIF images, when no significant signal is observed in the inner recirculation zone (RZ) (see Figure 1b) for the entire duration of the recording.

3. Results and Discussion

3.1 Fuel Penetration Depth

Figure 4 presents temporal mean Mie scattering images for $T_3 = T_{3,\mathrm{ref}}$. The analogous figures for other T_3 are omitted for brevity, but the trends are similar. The slight curving of the signal towards the centerline for $x/d_{\mathrm{bb}} > 1$, particularly at the lower FARs, is associated with the flow around the inner recirculation zone and contraction of this zone as LBO is approached. In bluff body combustors, the general flow pattern is as shown in Figure 1b (Lovett et al., 2011); previous particle image velocimetry measurements in this combustor are consistent with this image (Passarelli et al., 2023). Adopting terminology from Lovett et al. (2011), downstream of the inner RZ ($x/d_{\mathrm{bb}} > 1$ from Passarelli [2023] in this combustor) the flow enters a transition region, referred to as the close out region (COR). The streamlines in the COR initially converge towards the centerline of the bluff body, similar to the Mie signal behavior from $1 \lesssim x/d_{\mathrm{bb}} \lesssim 1.5$.

[1] Cantera is an open-source suite of tools for problems involving chemical kinetics, thermodynamics, and transport processes. Cantera is a sponsored project of NumFOCUS,® a 501(c) nonprofit charity in the United States. NumFOCUS is a registered trademark of NumFOCUS, Inc., Austin, Texas.

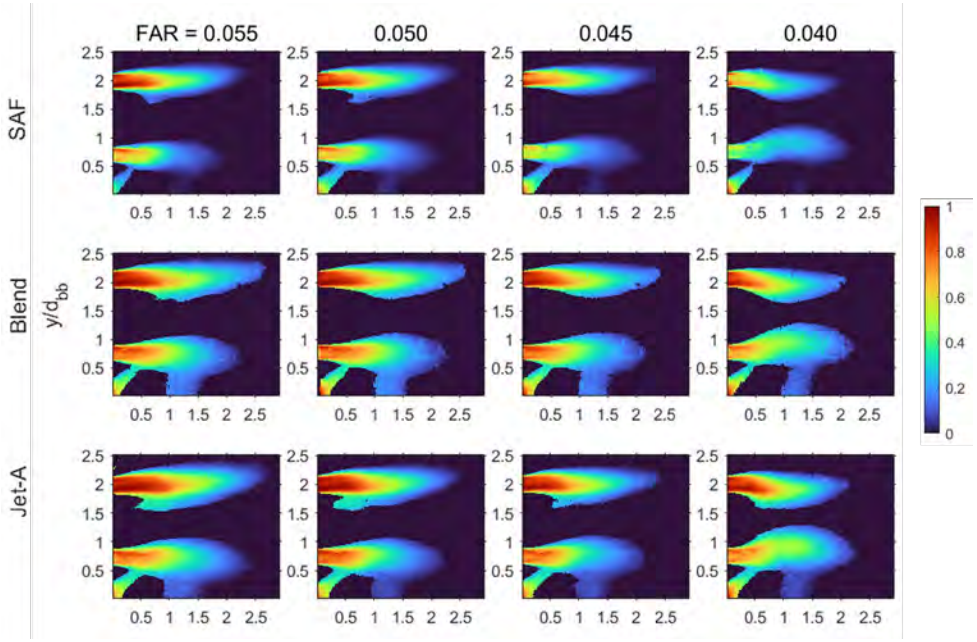

Figure 4. Temporal mean spray fields for $\boldsymbol{T_3 = T_{3,ref}}$ at nominal FARs. Colorbar represents a spray field normalized by the max intensity for presented test points. Flow progresses from left to right.

Figure 5 plots x_{dp} vs. FAR for all test conditions. As expected, higher T_3 lead to faster vaporization and lower penetration depths. Penetration depth also decreases with decreasing FAR due to the lower fuel flow rate that needs to be vaporized by the fixed air flow rate. Most notably, the SAF consistently has a lower penetration depth than the blend and fossil Jet A fuel. This is due to a combination of (i) lower surface tension promoting droplet breakup, (ii) higher vapor pressure indicating more volatility, and (iii) the distillation curve behavior, where the SAF showed the lowest boiling points of the fuels (see Table 2). Furthermore, the blend and fossil Jet A fuel have significant overlap, indicating that the less volatile components of the fossil fuel persist. The preferential vaporization of less volatile components of SAF/fossil blends has been observed previously but understanding its impact on combustion chemistry remains an open question (Xing et al., 2024).

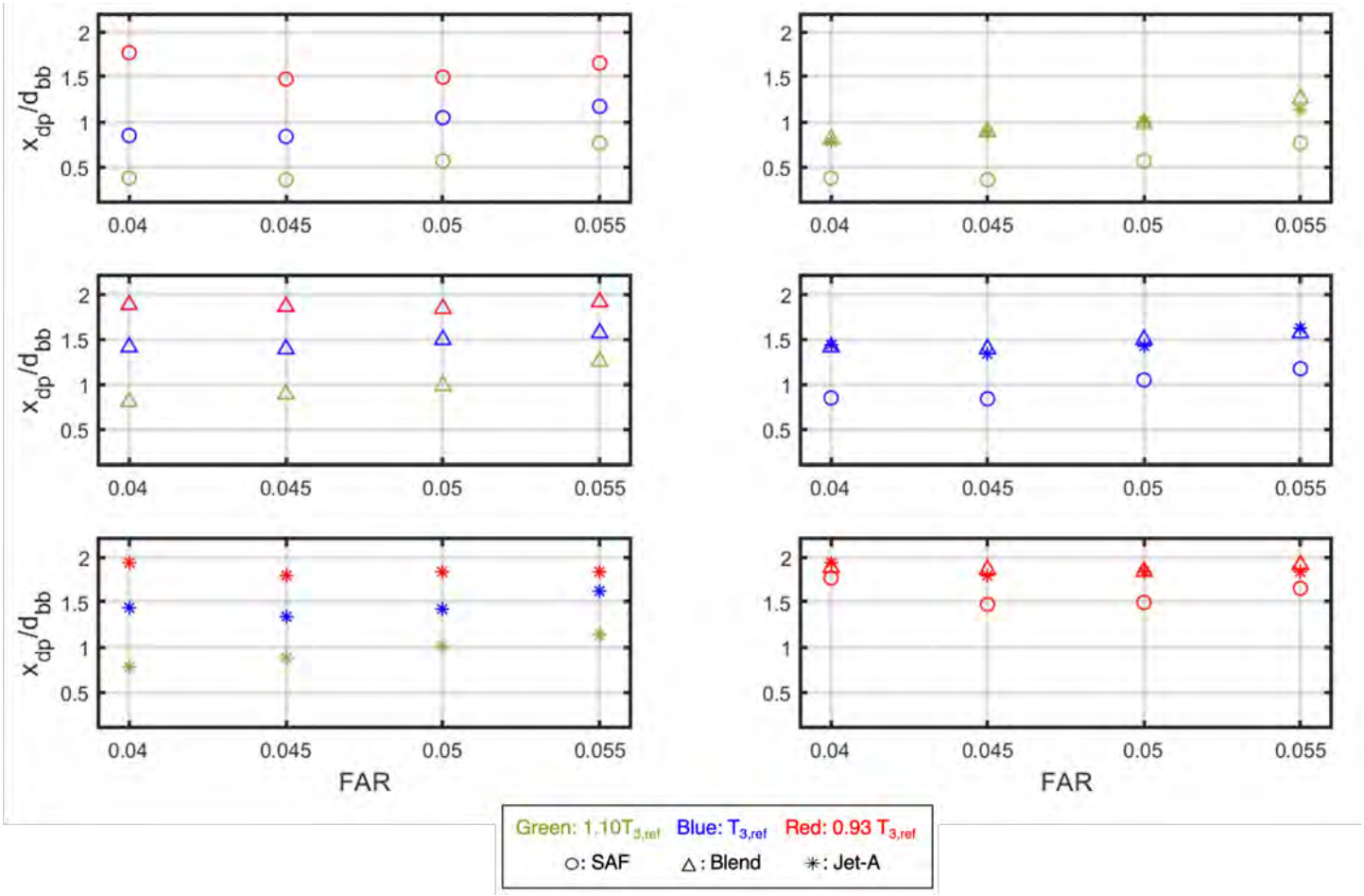

Figure 5. Penetration depth versus FAR for temperature sweeps by fuel (left) and fuel sweeps by temperature (right). Quantitative Droplet Characteristics.

A key objective of the PDPA campaign was to investigate the droplet size changes with reduction in FAR from the nominal value (i.e., 0.05) down to the blow off limit. In a previous campaign employing Jet A fuel, flame videos and OH* imaging showed that the flame transitions from attached at the mixer face to lifted once the FAR is reduced below FAR ~0.045. Therefore, in this study, we compare FAR of 0.040 and FAR of 0.050 cases to understand the droplet behavior at these extreme conditions. It should be mentioned that both the velocity and droplet size data are normalized for comparisons and absolute magnitudes can be made available upon request.

Velocity and droplet size results for the FAR variation at two axial locations, $x = 1$ mm and $x = 10$, are shown in Figure 6 and Figure 7. At $x = 1$ mm, the droplets concentrate mainly around the annular regions of the mains tubes. It should be noted that a significant number of droplets were found at the exit of the bluff body for the FAR = 0.040 case for the Jet A fuel because, at high FAR (>=0.045), the flame is attached to the mixer exit face and, therefore, most of the droplets are consumed by the flame. At low FARs, on the other hand, the flame is lifted and the droplets exiting the mixer are far from the reaction zone.

Figure 6 shows that the velocity profiles follow similar trends for all FARs and that their maximum magnitudes take place at the inner and outer shear layers of each tube, passing through a minimum somewhere between these two shear layers. Except for the FAR = 0.040 case, where the velocities are higher, the velocities look very similar for all the three cases. As the droplets move downstream, at $x = 10$ mm, the velocity profile changes and droplets are found for FAR = 0.050 along almost the entire vertical scan. Velocity magnitude, in all cases, was observed to be much higher than those at $x = 1$ mm. It should be noted that at $x = 10$ mm, the droplets coming from the pilot nozzle may confound the results. Overall, the

velocities of both fuels SAF and Jet A fuel behave in a similar way suggesting that the flow effect on the droplets is relatively similar for both fuels.

A key outcome of this work was to obtain droplet size for SAF and compare it to Jet A fuel. This is done in terms of profiles of the Sauter mean diameter D_{32}. The droplet size trends are shown in Figure 6e and Figure 6f. To help visualize the subtle differences, the top and bottom tube have been divided for $x = 1$ mm and are presented in a magnified view in Figure 7. Here we can see that the droplets show a minimum at the center of the annular regions and then quickly grow as they move to the edges and outside the annulus. There are some variations between the four annular regions, which could be due to variation in atomization caused by the difference in fueling between them. However, there is consistency between annular regions with respect to FAR dependency (i.e., the droplets decrease in size as the FAR decreases for a given fuel). This droplet size dependency with FAR has been observed before for other fuel nozzles tested in the same combustor. This is mainly due to a degradation in atomization as the fuel flow is increased while all other parameters are kept constant. Figure 7 shows that, at FAR = 0.040, the droplets near the bluff body region (Jet A fuel only) are much smaller is size than those in the annular regions. Typical droplet sizes are of the order of half the size of the droplets found in the annular main regions. At $x = 10$ mm (Figure 6), the droplets have decreased in size, which can be attributed to vaporization as they are convected downstream the flame. The higher FAR case had bigger droplets.

Comparing the SAF and Jet A fuel droplet sizes (Figure 6 and Figure 7) suggests that the SAF droplet size is smaller than that of Jet A fuel. Also, there are variations that seem to be jet dependent with the higher differences for the bottom jet, where Jet A fuel shows much bigger droplets. The droplet size trend with SAF is consistent with the Mie scattering measurements for the same operating conditions taken during the same campaign. The smaller droplet size for SAF can be explained in part by the physical properties of the fuel. That is, the fuel analysis performed by NREL, for the two fuels reported here, indicate that SAF has lower viscosity, surface tension, and boiling point. Therefore, for the same operating conditions, this could enable smaller droplets and faster vaporization as the fuel droplets convect towards the flame.

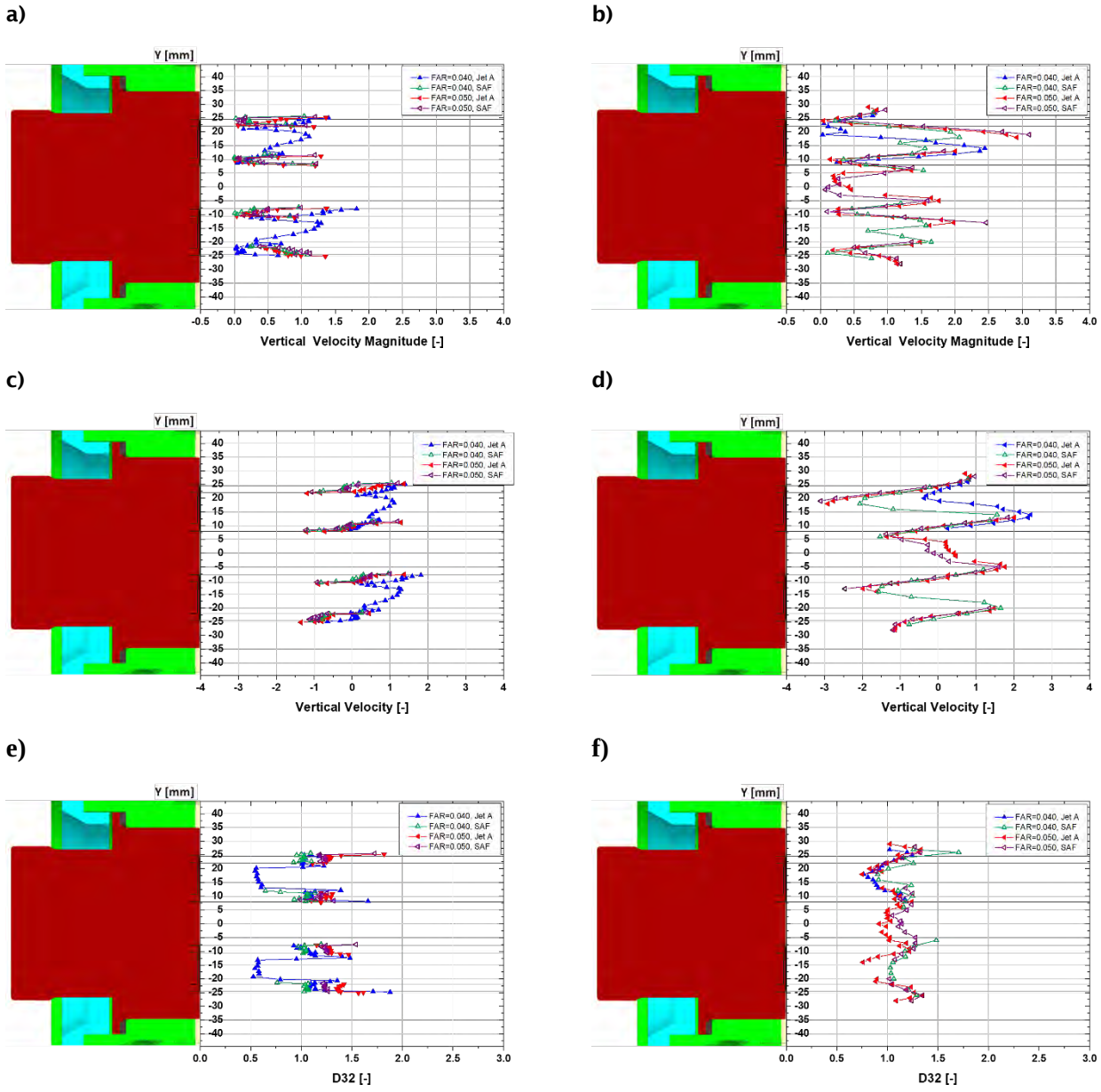

Figure 6. Impact of FAR on droplet speed, velocity, and size at two axial locations $x = 1$ mm (left column) and $x = 10$ mm (right column).

a)

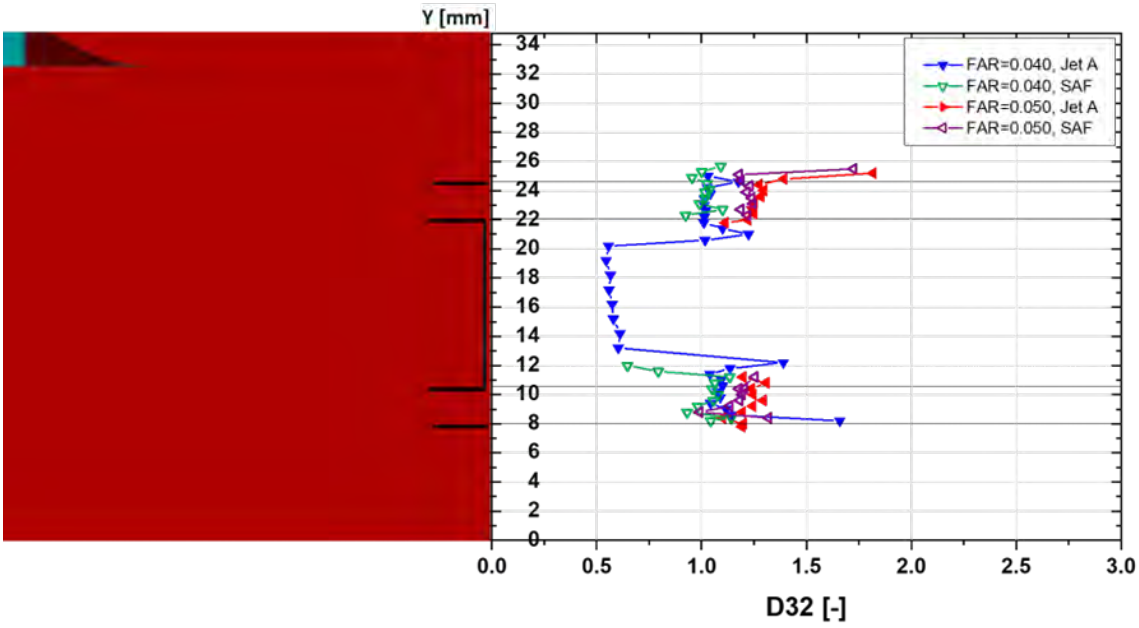

b)

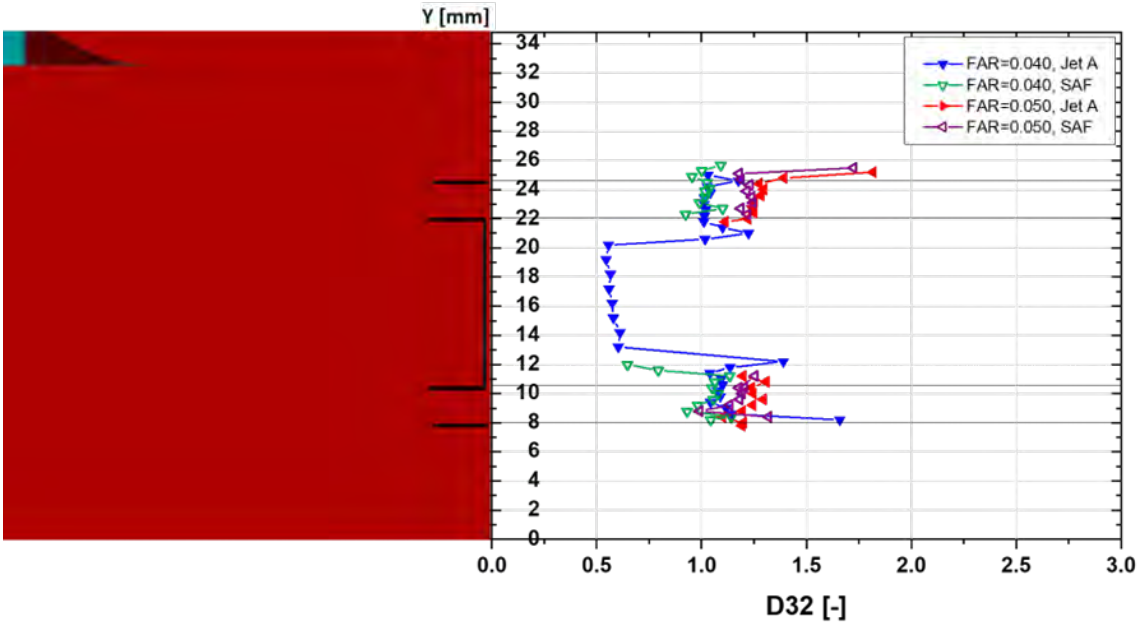

Figure 7. Impact of FAR on droplet size at axial location $x = 1$ mm showing a magnified view of the (a) top main tube and (b) bottom main tube.

The droplet size behavior as a function of T_3 is presented in Figure 8 and Figure 9. Figure 8 shows that, in general, the velocity follows similar trends, with the vertical coordinate, for both T_3 and fuels. At $x = 10$ mm, the velocities increase, and the velocity profiles seem to be more consistent for all cases. Magnified views of velocity are presented in Figure 9, showing smaller droplets at higher T_3s. This is expected because higher T_3 will increase the temperature difference that drives droplet vaporization. Regarding SAF and Jet A droplet differences, the SAF also shows consistently smaller droplets. The differences are also jet dependent with the highest differences observed for the bottom jet.

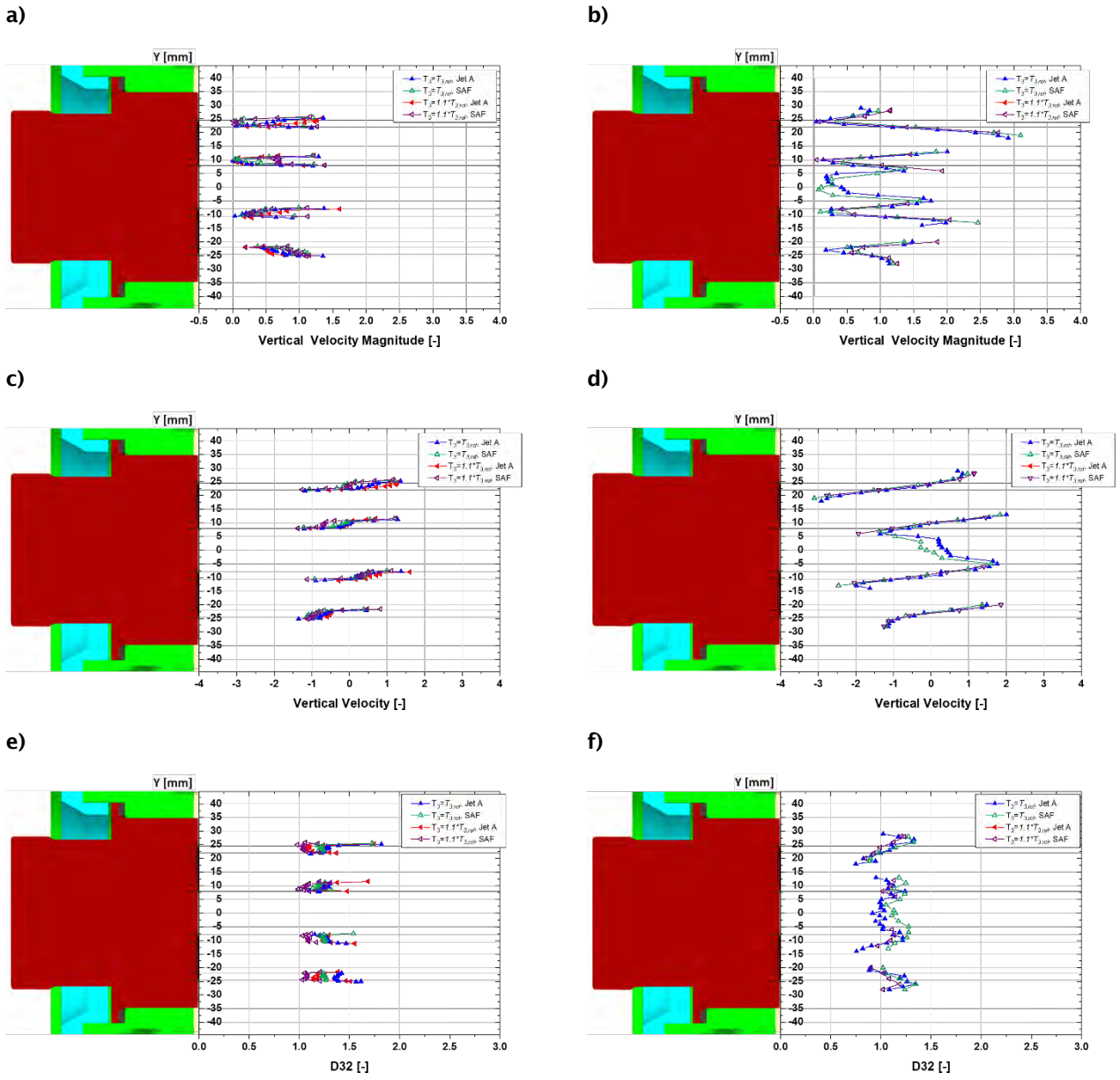

Figure 8. Impact of T_3 on droplet speed, velocity, and size at two axial locations $x = 1$ mm (left column) and $x = 10$ mm (right column).

a)

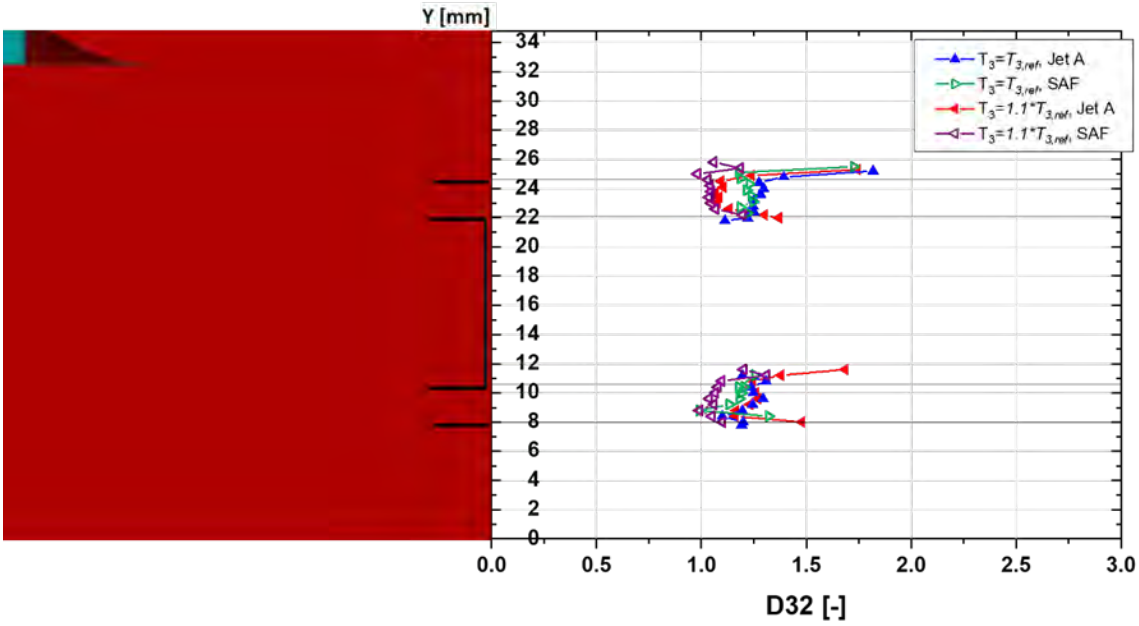

b)

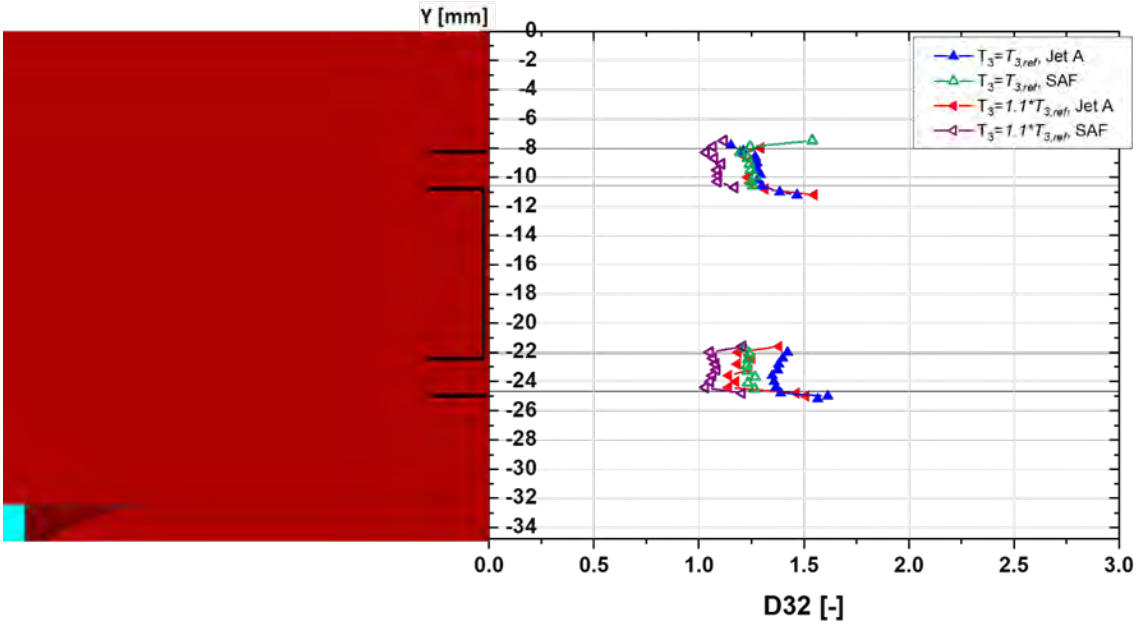

Figure 9. Impact of T_3 on droplet size at axial location $x = 1$ mm showing a magnified view of the (a) top main tube and (b) bottom main tube.

3.2 Flame Topology

The highly turbulent nature of the flow and flame is evident in the sample instantaneous OH PLIF image sequence in Figure 10. The image sequence also shows evidence of local extinction holes in the flame surface, consistent with approaching LBO (Shanbhogue et al., 2009). These holes allow for transport of mass and energy between reactants and products, and enhanced preheating and radical generation that have a favorable influence on the flame particularly in the inner RZ. As shown, the flame is able to "heal'" itself and remain attached.

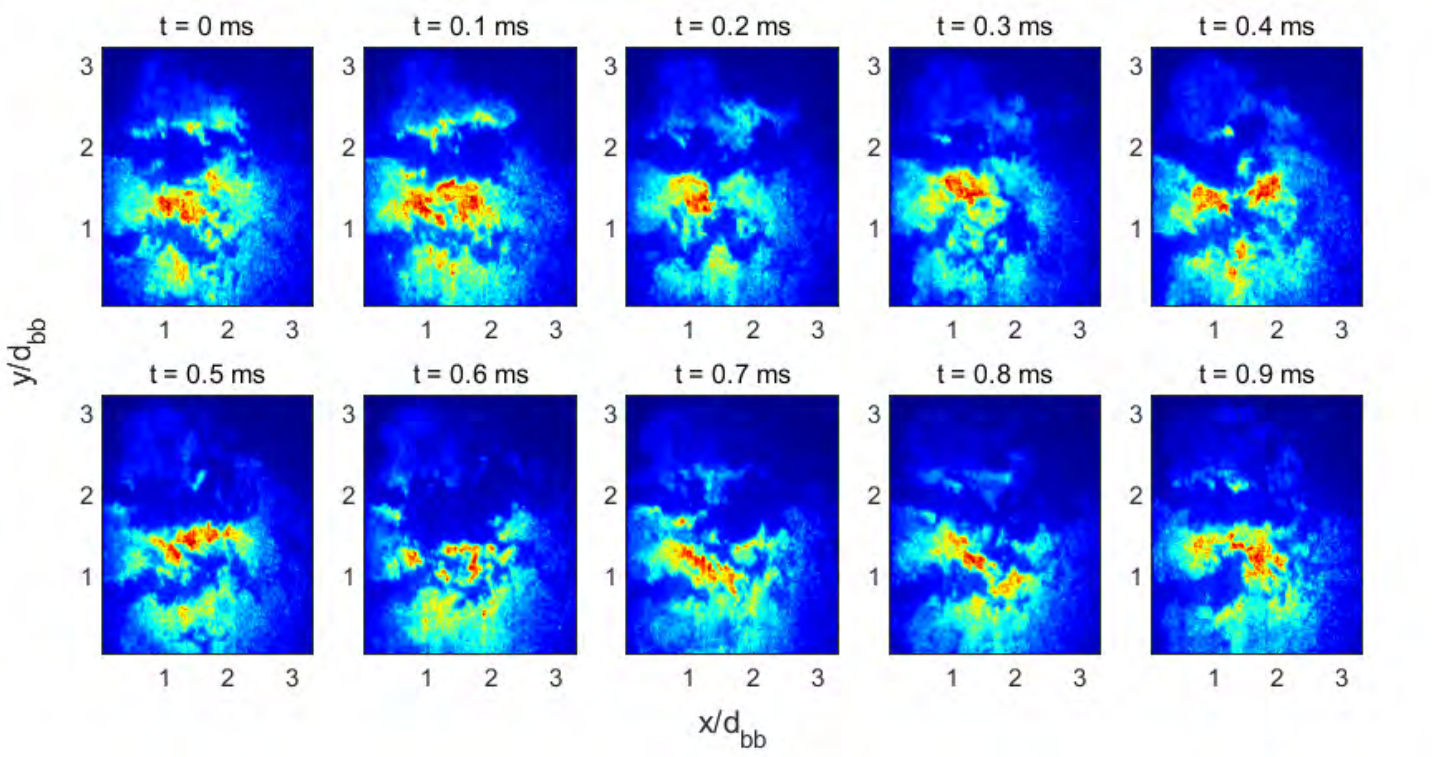

Figure 10. Instantaneous sequence of OH PLIF images for SAF, $\boldsymbol{T_3 = T_{3,\mathrm{ref}}}$ at FAR = 0.043. Flow from left to right.

Figure 11 presents 2D temporal mean FSD fields at $T_3 = T_{3,\mathrm{ref}}$ for varying FAR across all three fuels. Analogous figures for the other T_3 are omitted for brevity, but the fields and trends are similar. The FSD fields with the SAF consistently have higher values near the dome face for $x/d_{bb} < 0.5$. There is also a clear near-field reactant stream visible in the SAF that is less prevalent in the blend and Jet A fuel datasets. The Laser Induced Fluorescence (LIF) signal in this region is likely due to the aromatic content in the latter fuels, which is not present in the HEFA. Due to the varying fuel composition of kerosene fuels, the excitation of mono- and di-aromatics results in broadband fluorescence emission from 260-420 nm, which is resulting in crosstalk between fluorescence signals.

Referring to Figure 1b, the flame is anchored at the lip of the bluff body, and one observes the characteristic inner RZ directly downstream of the dome face. The flames are found in the shear layers surrounding the reactant streams where the boundary layers have separated from the edge of the bluff-body (Shanbhogue et al., 2009). As mentioned, downstream of the recirculation zone, the flow transitions from a recirculating flow to a wake flow. The transitional COR region features a convergence and then divergence of the flame surface from the centerline. Downstream of the COR, the flame surface diverges from the centerline due to entrainment.

As blow-off is approached (moving left to right in Figure 11), the recirculation zone becomes shorter in the x-direction, and the COR becomes thinner in the y-direction. The reduction of the recirculation zone is attributed to the reduced dilation rates (Tuttle, 2010). It has also been shown that as equivalence ratio drops and flame speed decreases, the flame moves closer to the unstable shear layer. The high strain rates in the shear layer can cause local extinction, as evidenced by the

holes in the flame. Eventually, excessive strain rates caused by shear layer vortices cause the flame sheet to become non-reactive, and the flame can no longer be sustained leading to blow-off (Chaudhuri et al., 2010).

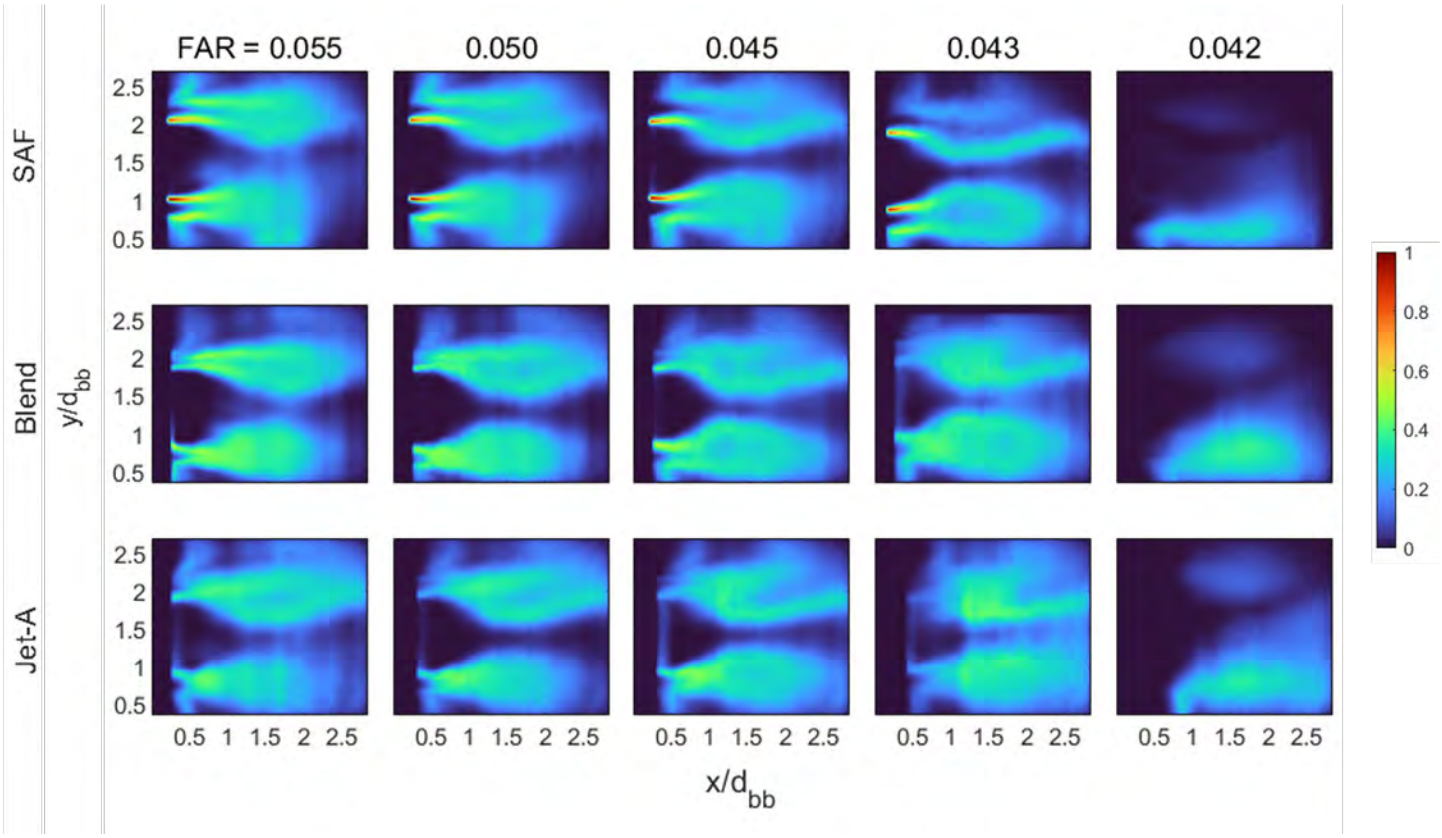

Figure 11. Temporal mean FSD fields for $T_3 = T_{3,\mathrm{ref}}$. Colorbar represents FSD normalized by the max FSD for presented test points. Flow progresses from left to right.

3.3 Blow-off Behavior

It previously was shown that differing physical fuel properties caused systematic differences in fuel penetration depth. As mentioned, the physics limiting processes for LBO due to fuel property affects are said to be governed by a competition between mixing/evaporation rate and chemical kinetic rate (Colket & Heyne, 2021). When fuel/air mixing occurs rapidly relative to the combustion chemistry or has already occurred prior to combustion as in LPP systems, LBO is kinetically limited and vaporization/mixing disparities we observed may be insignificant. The HEFA has a higher H/C ratio, LHV, and indicated cetane number (ICN), which suggests that it may be more resistant to blow-off (Rock et al., 2019). However, Table 3 show no significant trends at a given T_3.

Table 3. LBO FAR for different T_3 and fuel.

	HEFA	Blend	Jet A
$0.93T_{3,\mathrm{ref}}$	0.044±0.0003	0.045±0.0003	0.043±0.0003
$T_{3,\mathrm{ref}}$	0.042±0.0004	0.042±0.0004	0.042±0.0004
$1.10T_{3,\mathrm{ref}}$	0.039±0.0004	0.040±0.0004	0.039±0.0004

These similarities can be explained by blow-off Damköhler vs. Reynolds number correlations detailed earlier. First examining Re for a given T_3, primary disparities between fuels would be due to varying ρ_3 and μ_3, as $\dot{m}_{\mathrm{main}}$ is kept constant

for each fuel. However, due to the very lean nature of the mixture, these differences are minimal and therefore Re_{LBO} is approximately the same across fuels. For Da_{LBO}, it then follows that τ_f would also be approximately constant.

Additionally, δ_f^0 and S_L^0 in τ_c did not significantly vary across fuels. Experiments in previous studies have also shown that S_L^0 between HEFA blends and Jet A fuel are similar (Munzar et al., 2014; Hui et al., 2012). S_L^0 has a strong dependence on adiabatic flame temperature, which is directly controlled by LHV (Hui et al., 2012). While the LHV of the HEFA is slightly higher than the Jet A fuel, the difference is not significant enough to have meaningful impacts on S_L^0.

Figure 12 presents the LBO limits in the current experiments against data from the literature (Shanbhogue et al., 2009) for axisymmetric bluff bodies. The data from this study (blue dots), and previous campaigns (orange dots) are grouped towards the lower limit, indicating more robustness to LBO. The blow-off results across fuels are therefore encouraging for further applications of this combustor and LPP.

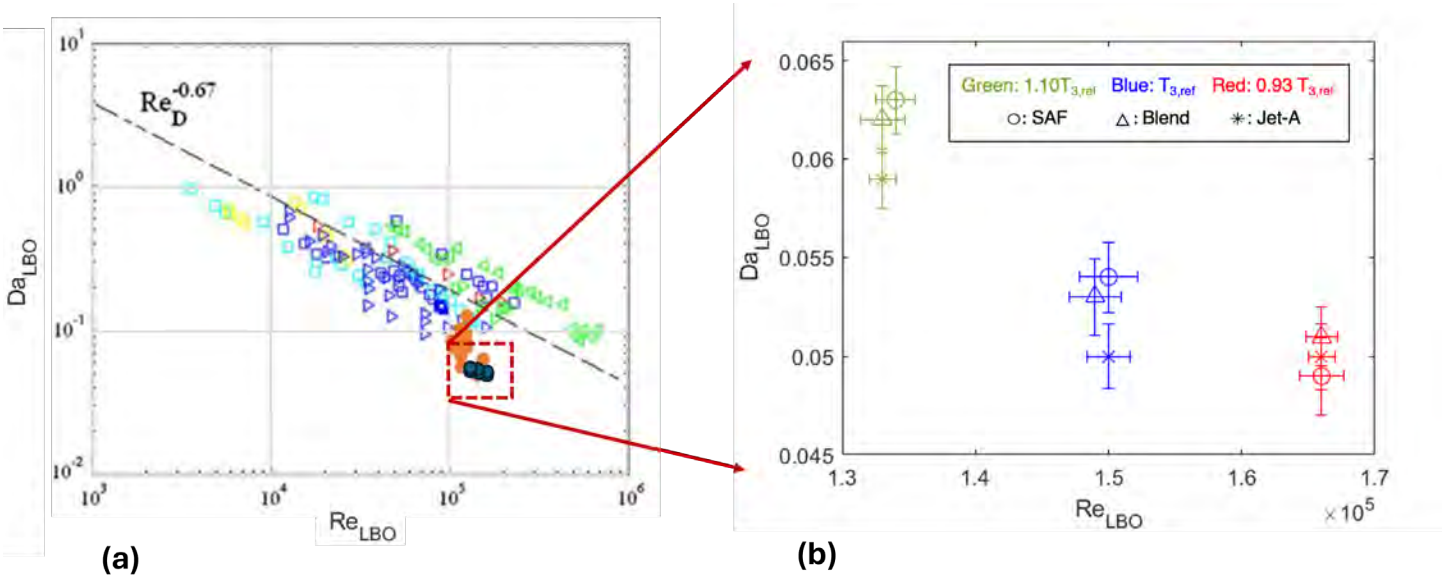

Figure 12. Blow-off Damköhler number (Da) vs. Reynolds number (Re). (a) Data from this study (solid blue) overlayed on axisymmetric bluff bodies from Shanbhogue et al. (2009). (b) Detailed view of blow-off Damköhler number vs. Reynolds number for the current study.

Milestones

- Completed campaign 3.
- Completed data analysis from campaign 3.

Major Accomplishments

- Measured the impact of fuel properties on spray characteristics.
- Measured the flame structure and FSD fields in LPP combustor.
- Demonstrated robust operation with SAF, despite atomization/vaporization differences.
- Established LBO correlation based on Damköhler and Reynolds numbers for LPP combustor, including SAF.

Publications

Jain, A., Obi, I., Mazumdar, Y. C., Salazar, V., Kodali, M., Venkatesan, K., & Steinberg, A. M. (In preparation). Flame structure, spray, and blowout of a lean premixed prevaporized combustor with conventional and sustainable jet fuels. *AIAA Journal*.

Jain, A., Obi, I., Mazumdar, Y. C., Salazar, V., Kodali, M., Venkatesan, K., & Steinberg, A. M. (2025, January 6-10). *Flame structure, spray, and blowout of a lean premixed prevaporized combustor with conventional and sustainable jet fuels* [Conference paper]. AIAA SCITECH 2025 Forum, Orlando, Florida.

Passarelli, M. L., Wonfor, S. E., Zheng, A. X., Mazumdar, Y., Steinberg, A. M., Bower, H., Hong, J., & Venkatesan, K. (2024, June 24-28). *Blowoff characteristics of a bluff-body stabilized, multi-element, lean premixed pre-vaporized combustor for supersonic transport applications* [Conference paper]. ASME Turbo Expo 2024: Turbomachinery Technical Conference and Exposition, London, United Kingdom. https://doi.org/10.1115/GT2024-129322

Zheng, A. X., Manikandan, S. R., Wonfor, S. E., Steinberg, A. M., & Mazumdar, Y. C. (2023). Planar time-resolved laser-induced incandescence for pressurized premixed Jet A combustion. *Applied Physics B: Lasers and Optics, 129*(71).

Salazar, V., Venkatesan, K., Han, F., Wonfor, S., Passarelli, M., Zheng, A., & Steinberg, A. M. (2023, January 26-30). *Acoustic and optical flame transfer function measurements in a high-pressure lean-burn aero-engine combustor fueled with Jet A* [Conference paper]. ASME Turbo Expo 2023: Turbomachinery Technical Conference and Exposition, Orlando, Florida. https://doi.org/10.1115/GT2023-103222

Passarelli, M. L., Wonfor, S. E., Zheng, A. X., Mazumdar, Y. C., Seitzman, J. M., Steinberg, A. M., Salazar, V., Venkatesan, K., & Benjamin, M. (2023). *Forced and unforced dynamics of a lean premixed prevaporized combustor for civil supersonic transport* [Conference paper]. AIAA SCITECH 2023 Forum, National Harbor, Maryland. https://doi.org/10.2514/6.2023-0920

Passarelli, M. L., Wonfor, S., Zheng, A. X., Manikandan, S. R., Mazumdar, Y. C., Seitzman, J. M., Steinberg, A. M., Bower, H., Hong, J., Venkatesan, K., & Benjamin, M. (2022, January 3-7). *Experimental characterization of a lean prevaporized premixed combustor for supersonic transport applications* [Conference presentation]. AIAA SCITECH 2022 Forum, San Diego, California. https://doi.org/10.2514/6.2022-2347

Student Involvement
Arihant Jain (PhD Student), Ijeoma Obi (MS Student), Mitchell Passarelli (PhD Student, graduated) contributed to this task.

Awards
None.

Plans for Next Period
Task 1 is complete. The effort to further advance LPP combustion will continue under ASCENT Project 098, focused on advancing the technology readiness level (TRL) for subsonic aircraft engines.

Task 2 - Computational Simulations of Combustor
Georgia Institute of Technology

Objective
The objective of this task is to develop and validate best practices for industry-scale simulations of LPP combustion. This involves a combination of industry- and research-scale CFD simulations, predominantly using LES.

Research Approach
To benchmark current CFD approach against experimental data, unsteady CFD simulations were performed for experimental conditions explored during Year 2 (2022-2023). Predictions from the industrial scale LES simulations were compared against the experimental measurements of 2D fuel-air mixing, 2D combustor heat release imaging and droplet sizing from phase Doppler Interferometry. Based on comparison of CFD to experimental data at two different FARs, it was concluded that the initially assumed droplet distribution, as well as accurate modelling of evaporation and fuel-air mixing, are key to better matching with observed experimental trends. The computational fuel injection model likely needs further improvement, requiring a better definition of fuel evolution at the injection boundary for better prediction of the amount of liquid versus vapor fuel at combustor inlet. Also, boundary conditions from the CFD simulations were provided to the NREL for reduced domain modelling and code-code comparison, as part of benchmarking the industrial scale simulations against state-of-the-art high-fidelity simulations.

The activity in 2023 helped identify deficiencies in the liquid fuel injection method employed in the CFD simulations. To address the inadequacy, the computational team is investigating a high-fidelity fuel injection process based on a hybrid volume of fluid (VoF)/discreet particle method (DPM) approach. The idea is to generate the fuel-injection by employing a sub-model and, additionally, to run the full-model unsteady CFD simulation using VoF based fuel-injection. Unsteady CFD simulations at Year 2 experimental conditions with the high-fidelity injection process are in progress and will be compared and contrasted against the previous CFD and experimental measurements.

The industrial-scale LES of the burner has been completed. The high-fidelity LES being conducted by NREL is ongoing under U.S. Department of Energy funding. The project team will continue to collaborate with NREL regarding boundary conditions and validation data.

Milestones

- Completed the LES of Year 2 conditions using industry-scale simulations.
- Transmitted the boundary conditions for high-fidelity simulations
- Established a hybrid fuel injection model.
- Obtained and processed spray, flame, and velocity data for simulation validation.

Major Accomplishments

- Identified changes in boundary conditions required for more accurately simulating LPP fuel injection.
- Progressed a partnership with NREL.

Publications

None.

Student Involvement

Arihant Jain (PhD Student), Ijeoma Obi (MS Student), Mitchell Passarelli (PhD Student, graduated) contributed to this task.

Awards

None.

Plans for Next Period

Task 2 is complete. The effort to further advance LPP combustion will continue under ASCENT Project 098, focused on advancing the TRL for subsonic aircraft engines. The NREL team will continue the high-fidelity LES that is being conducted under DoE funding. The ASCENT Project 074 team will continue to work with NREL to assess the simulations against the experimental data.

Task 3 - Analysis of Thermoacoustic Dynamics

Georgia Institute of Technology

Objectives

The objectives of this activity were to (1) measure the forced response of the LPP combustor to acoustic perturbations, (2) model the response using GE's thermoacoustic solver tools, (3) improve and validate these tools, as appropriate, and (4) physically explain the processes leading to thermoacoustic dynamics in this experiment.

Research Approach

Due to timing of the reports, proposal approvals, and no-cost extensions, the thermoacoustic measurement and modeling tasks were completed prior to the previous ASCENT Project 074 report. No further activities were required during this past performance period to complete the task objectives.

Milestones

- Completed the measurement of flame transfer functions.
- Completed the analysis of forced experimental results.
- Completed the preliminary analysis of flame transfer functions using network modeling.

Major Accomplishments

- Performed the first measurements of flame transfer functions and forced response of this type of LPP combustor.

Publications

None.

Student Involvement

Mitchell Passarelli (PhD Student, graduated) contributed to this task.

Awards

None.

Plans for Next Period

Task 3 is complete. The effort to further advance LPP combustion will continue under ASCENT Project 098, focused on advancing the TRL for subsonic aircraft engines.

References

ASTM International. (2023). ASTM D1655-22a: Standard specification for aviation turbine fuels. https://doi.org/10.1520/D1655-22A

Bell, J. B., Day, M. S., Grcar, J. F., Lijewski, M. J., Driscoll, J. F., & Filatyev, S. A. (2007). Numerical simulation of a laboratory-scale turbulent slot flame. *Proceedings of the Combustion Institute, 31*(1), 1299–1307. https://doi.org/10.1016/j.proci.2006.07.186

Berton, J. J., Huff, D. L., Geiselhart, K., & Seidel, J. (2020). Supersonic technology concept aeroplanes for environmental studies. In *AIAA Scitech 2020 Forum* (p. 0263).

Candel, S. M., & Poinsot, T. J. (1990). Flame stretch and the balance equation for the flame area. *Combustion Science and Technology, 70*(1-3), 1–15. https://doi.org/10.1080/00102209008951608

Canny, J. (1986). A computational approach to edge detection. *IEEE Transactions on Pattern Analysis and Machine Intelligence, PAMI-8*(6), 679–698. https://doi.org/10.1109/TPAMI.1986.4767851

Carter, C. D., & Lee, T. (2022). LIF theory and practice (Ch. 5, pp. 181–254). In A. Steinberg & S. Roy (Eds.), *Optical Diagnostics for Reacting and Non-reacting Flows: Theory and Practic*e. American Institute of Aeronautics and Astronautics, Reston, Virginia.

Cavaliere, D. E., Kariuki, J., & Mastorakos, E. (2013). A comparison of the blow-off behaviour of swirl-stabilized premixed, non-premixed and spray flames. *Flow, Turbulence and Combustion, 91*(2), 347–372. https://doi.org/10.1007/s10494-013-9470-z

Chaib, O., Zheng, Y., Hochgreb, S., & Boxx, I. (2023). Hybrid algorithm for the detection of turbulent flame fronts. *Experiments in Fluids, 64*(5), 104. https://doi.org/10.1007/s00348-023-03651-6

Chaudhuri, S., Kostka, S., Renfro, M. W., & Cetegen, B. M. (2010). Blowoff dynamics of bluff body stabilized turbulent premixed flames. *Combustion and Flame, 157*(4), 790–802. https://doi.org/10.1016/j.combustflame.2009.10.020

Colket, M., & Heyne, J. (2021). *Fuel effects on operability of aircraft gas turbine combustors*. Progress in Astronautics and Aeronautics, American Institute of Aeronautics and Astronautics, Reston, Virginia.

Dooley, S., Won, S. H., Chaos, M., Heyne, J., Ju, Y., Dryer, F. L., Kumar, K., Sung, C.-J., Wang, H., Oehlschlaeger, M. A., Santoro, R. J., & Litzinger, T. A. (2010). A jet fuel surrogate formulated by real fuel properties. *Combustion and Flame, 157*(12), 2333–2339. https://doi.org/10.1016/j.combustflame.2010.07.001

EPA. (2007). *Methodology for thermal efficiency and energy input calculations and analysis of biomass cogeneration unit characteristics* (EPA-HQ-OAR-2007-0012). U.S. Environmental Protection Agency (EPA). https://www3.epa.gov/ttn/atw/utility/fnl_biomass_cogen_TSD_04_19_07.pdf

Filatyev, S. A., Driscoll, J. F., Carter, C. D., & Donbar, J. M. (2005). Measured properties of turbulent premixed flames for model assessment, including burning velocities, stretch rates, and surface densities. *Combustion and Flame, 141*(1), 1–21. https://doi.org/10.1016/j.combustflame.2004.07.010

Fugger, C. A., Hsu, P. S., Jiang, N., Yi, T., Slipchenko, M. N., Felver, J. J., Smith, T. E., Emerson, B. L., Lieuwen, T. C., & Roy, S. (2020). 10-kHz simultaneous dual-plane stereo-PIV and OH-PLIF imaging. *Applied Physics B, 126*(10), 167. https://doi.org/10.1007/s00340-020-07522-4

Han, D., Satija, A., Gore, J. P., & Lucht, R. P. (2018). Experimental study of CO_2 diluted, piloted, turbulent CH_4/air premixed flames using high-repetition-rate OH PLIF. *Combustion and Flame, 193*, 145–156. https://doi.org/10.1016/j.combustflame.2018.03.012

Hassan, M., Pfaender, H., & Mavris, D. (2020). Design tools for conceptual analysis of future commercial supersonic aircraft. In *AIAA Aviation 2020 Forum* (p. 2620).

Hui, X., Kumar, K., Sung, C.-J., Edwards, T., & Gardner, D. (2012). Experimental studies on the combustion characteristics of alternative jet fuels. *Fuel, 98*, 176–182. https://doi.org/10.1016/j.fuel.2012.03.040.13

Kharina, A., MacDonald, T., & Rutherford, D. (2018, July). Environmental performance of emerging supersonic transport aircraft. ICCT.

Liang, Y., Liu, X., Yang, M., Hui, X., & Wang, J. (2024). Investigating the oxidation characteristic of a hydro-processed bio-jet fuel: Experimental and modeling study. *Combustion and Flame, 270*, 113778. https://doi.org/10.1016/j.combustflame.2024.113778

Lovett, J. A., Cross, C., Lubarsky, E., & Zinn, B. T. (2011, June 6-10). *A review of mechanisms controlling bluff-body stabilized flames with closely-coupled fuel injection* [Conference paper]. ASME 2011 Turbo Expo: Turbine Technical Conference and Exposition, Vancouver, British Columbia. https://doi.org/10.1115/GT2011-46676

Munzar, J. D., Zia, A., Versailles, P., Jiménez, R., Bergthorson, J. M., & Akih-Kumgeh, B. (2014, June 16-20). C*omparison of laminar flame speeds, extinction stretch rates and vapor pressures of Jet A-1/HRJ biojet fuel blends* [Conference paper]. ASME Turbo Expo 2014: Turbine Technical Conference and Exposition, Düsseldorf, Germany. https://doi.org/10.1115/GT2014-25951

Niedzwiecki, R. W. (1992, April). Low emissions combustor technology for high-speed civil transport engines. In *NASA. Langley Research Center, First Annual High-Speed Research Workshop, Part 2*.

Passarelli, M. (2023). *An experimental characterization of a multi-element lean premixed pre-vaporized combustor for supersonic transport applications* [Doctoral dissertation, Georgia Institute of Technology]. Georgia Institute of Technology

Passarelli, M. L., Wonfor, S. E., Zheng, A. X., Mazumdar, Y., Steinberg, A. M., Bower, H., Hong, J., & Venkatesan, K. (2024, June 24-28). *Blowoff characteristics of a bluff-body stabilized, multi-element, lean premixed pre-vaporized combustor for supersonic transport applications* [Conference paper]. ASME Turbo Expo 2024: Turbomachinery Technical Conference and Exposition, London, United Kingdom. https://doi.org/10.1115/GT2024-129322

Passarelli, M. L., Wonfor, S. E., Zheng, A. X., Mazumdar, Y. C., Seitzman, J. M., Steinberg, A. M., Salazar, V., Venkatesan, K., & Benjamin, M. (2023). *Forced and unforced dynamics of a lean premixed prevaporized combustor for civil supersonic transport* [Conference paper]. AIAA SCITECH 2023 Forum, National Harbor, Maryland. https://doi.org/10.2514/6.2023-0920

Passarelli, M. L., Wonfor, S., Zheng, A. X., Manikandan, S. R., Mazumdar, Y. C., Seitzman, J. M., Steinberg, A. M., Bower, H., Hong, J., Venkatesan, K., & Benjamin, M. (2022, January 3-7). *Experimental characterization of a lean prevaporized premixed combustor for supersonic transport applications* [Conference paper]. AIAA SCITECH 2022 Forum, San Diego, California. https://doi.org/10.2514/6.2022-2347

Ranzi, E., Frassoldati, A., Stagni, A., Pelucchi, M., Cuoci, A., & Faravelli, T. (2014). Reduced kinetic schemes of complex reaction systems: Fossil and biomass-derived transportation fuels. *International Journal of Chemical Kinetics, 46*(9), 512–542. https://doi.org/10.1002/kin.20867

Rock, N., Chterev, I., Emerson, B., Won, S. H., Seitzman, J., & Lieuwen, T. (2019). Liquid fuel property effects on lean blowout in an aircraft relevant combustor. *Journal of Engineering for Gas Turbines and Power, 141*, 071005. https://doi.org/10.1115/1.4042010

Saini, P., Chterev, I., Pareja, J., Aigner, M., & Boxx, I. (2020). Effect of pressure on hydrogen enriched natural gas jet flames in crossflow. *Flow, Turbulence and Combustion, 105*(3), 787–806. https://doi.org/10.1007/s10494-02000148-8

Salazar, V., Venkatesan, K., Han, F., Wonfor, S., Passarelli, M., Zheng, A., & Steinberg, A. M. (2023, January 26-30). *Acoustic and optical flame transfer function measurements in a high-pressure lean-burn aero-engine combustor fueled with Jet A* [Conference paper]. ASME Turbo Expo 2023: Turbomachinery Technical Conference and Exposition, Orlando, Florida. https://doi.org/10.1115/GT2023-103222

Shanbhogue, S. J., Husain, S., and Lieuwen, T. (2009). Lean blowoff of bluff body stabilized flames: Scaling and dynamics. *Progress in Energy and Combustion Science, 35*(1), 98–120. https://doi.org/10.1016/j.pecs.2008.07.003

Speth, R. L., Eastham, S. D., Fritz, T. M., Sanz-Morere, I., Agarwal, A., Prashanth, P., ... & Barrett, S. R. (2021). *Global environmental impact of supersonic cruise aircraft in the stratosphere* (No. E-19920).

Sweeney, M., & Hochgreb, S. (2009). Autonomous extraction of optimal flame fronts in OH planar laser-induced fluorescence images. *Applied Optics, 48*(19), 3866–3877. https://doi.org/10.1364/AO.48.003866

Tuttle, S. G. (2010). *Blowoff behavior of bluff body stabilized flames in vitiated and partially premixed flows* [Doctoral dissertation, University of Connecticut]. University of Connecticut ProQuest Dissertations & Theses, 3428890. https://doi.org/https://www.proquest.com/dissertations-theses/blowoff-behavior-bluff-bodystabilized-flames/docview/757375950/se-2

Vozka, P., Šimáček, P., & Kilaz, G. (2018). Impact of HEFA feedstocks on fuel composition and properties in blends with Jet A. *Energy & Fuels, 32*(11), 11595–11606. https://doi.org/10.1021/acs.energyfuels.8b02787

Xing, J., An, Z., & Kurose, R. (2024). Analysis and flamelet modeling of preferential evaporation in SAF/Jet A spray flames. *Proceedings of the Combustion Institute, 40*(1–4), 105707. https://doi.org/10.1016/j.proci.2024.105707